# Chiral Partition Functions
# of Quantum Hall Droplets

Andrea CAPPELLI

*INFN*

*Via G. Sansone 1, 50019 Sesto Fiorentino - Firenze, Italy*

Giovanni VIOLA

*INFN and Dipartimento di Fisica*

*Via G. Sansone 1, 50019 Sesto Fiorentino - Firenze, Italy*

Guillermo R. ZEMBA

*Facultad de Ciencias Fisicomatemáticas e Ingeniería, UCA*

*Av. A. Moreau de Justo 1500, (1107) Buenos Aires, Argentina*

*and Departamento de Física, CNEA*

*Av.Libertador 8250, (1429) Buenos Aires, Argentina*

**Abstract**

Chiral partition functions of conformal field theory describe the edge excitations of isolated Hall droplets. They are characterized by an index specifying the quasiparticle sector and transform among themselves by a finite-dimensional representation of the modular group. The partition functions are derived and used to describe electron transitions leading to Coulomb blockade conductance peaks. We find the peak patterns for Abelian hierarchical states and non-Abelian Read-Rezayi states, and compare them. Experimental observation of these features can check the qualitative properties of the conformal field theory description, such as the decomposition of the Hilbert space into sectors, involving charged and neutral parts, and the fusion rules.

# 1 Introduction

## 1.1 Disk partition functions

Within the conformal field theory description of edge excitations [1][2], the advanced methods of rational conformal field theories (RCFT) [3] have been recently applied to discuss the interference of non-Abelian anyons [4][5] and to determine the bipartite entanglement entropy of topological ordered ground states [6]. The RCFT methods, and the corresponding properties of topological Chern-Simons gauge theories, were originally investigated by Verlinde [7], Witten [8], Moore and Seiberg and others [9]. These authors analyzed the equations of crossing symmetry (duality) of $n$-point correlators and the identities relating these functions among themselves on general Riemann surfaces. The fundamental sets of relations were shown to be: i) the modular invariance of the partition functions (1-point functions) on the toroidal geometry; ii) the crossing symmetry of the 4-point function on the sphere. All other equations follow by "sewing" the surfaces with handles and punctured spheres [9].

The rational theories are characterized by a finite set of quasiparticle excitations with rational values of spin and statistics (scaling dimensions). The prominent theories of the quantum Hall effect are indeed RCFTs: the Abelian states, which are (multicomponent) Luttinger liquids described by charge lattices [10], and the non-Abelian Read-Rezayi states [11], that involve $\mathbb{Z}_k$ parafermions [12]. Other theories, such as the $W_{1+\infty}$ models [13] and the Fradkin-Lopez theory [14] for the Jain states [15], are not rational theories but projections of them, such that their properties can be traced back to those of RCFTs. Therefore, the rational CFTs are of general physical interest.

In the recent literature, the RCFT methods have been reconsidered and extended [16][5]: the duality equations for four and higher-point functions have been thoroughfully analyzed, in particular for studying interferometry of non-Abelian anyons [4]. On the other hand, the modular invariant partition functions have not been extensively discussed.

In this paper, we provide a rather complete and selfcontained discussion of the partition functions in the QHE setting. Based on a previous study of partition functions on the annulus geometry [17], we obtain the chiral partition functions that pertain to the disk geometry and study their properties [18]. These partition functions describe the excitations of isolated droplets of Hall fluid and provide a complete definition of their Hilbert space and its decomposition into sectors; moreover, the fusion rules, the selection rules for the composition of excitations, are built in.

The general form of the annulus partition function is:

$$Z_{\text{annulus}} = \sum_{\lambda=1}^{N} \theta_\lambda \, \overline{\theta}_\lambda \, , \qquad (1.1)$$

where the index $\lambda$ runs over the sectors of the theory, described by the functions $\theta_\lambda$,

that are analytic (resp. anti-analytic) for the inner (resp. outer) edge.

The annulus partition function is defined on the spacetime torus made by the edge circle and the compact Euclidean time: it is invariant under modular transformations, the discrete coordinate reparametrizations that respect the double periodicity of the torus geometry [3]. In RCFTs, modular invariance is achieved as follows: the generalized theta functions $\theta_\lambda$ transform by a unitary linear representation of dimension $N$, that leaves the sesquilinear form (1.1) invariant. An interesting feature is that the number of sectors $N$ is equal to Wen's topological order [1], the degeneracy of Hall ground states on the compact toroidal space (a general proof of this result is reported in section 2.2 of [17]). Another fact is that the states in each $\lambda$ sector form a representation of the maximal chiral algebra of the RCFT, whose character is $\theta_\lambda$.

In section 2, we introduce the annulus partition functions in the simpler case of Laughlin plateaux, with filling fraction $\nu = 1/p$ ($p$ odd); we describe the conditions of modular invariance and solve them to obtain the form (1.1) with $N = p$. We show that the geometrical modular conditions have clear physical meanings in the QHE setting and provide useful building principia. In the Laughlin case, the characters $\theta_\lambda$ resum all excitations with same fractional charge part, $Q = \lambda/p + \mathbb{Z}$: the corresponding chiral algebra is the extension of $\widehat{U(1)}$ current algebra (Luttinger theory) by a field of scaling dimension $h = p/2$; the fusion rules for the corresponding excitations are given by the additive group $\mathbb{Z}_p$.

In Section 2.3, the disk partition functions are obtained by taking the limit of $Z_{\text{annulus}}$ when the inner circle shrinks to zero, leading to:

$$Z_{\text{disk}}^{(\alpha)} = \theta_\alpha \ , \tag{1.2}$$

where the sector $\lambda = \alpha$ is chosen according to the type of quasiparticles in the bulk [18][19]. Besides the Laughlin case, in this paper we provide the expressions of $Z_{\text{disk}}$ for general multicomponent Luttinger liquid theories, including the Jain states, and for the non-Abelian Read-Rezayi states, using new and known results of the corresponding annulus partition functions [17][20].

## 1.2   Coulomb blockade in quantum Hall droplets

In Fig. 1 is drawn the geometry of the quantum Hall interferometer, namely a bar-shaped sample with two constrictions [21]. In this device, one can consider two opposite regimes of weak and strong backscattering of edge excitations at the constrictions: the interference of edge waves is best achieved in the weak backscattering limit $(a)$, while the Coulomb blockade takes place for strong backscattering $(b)$. In the latter limit, an isolated droplet of Hall fluid is formed and only electrons can tunnel into the droplet. The electric potential difference is counterbalanced by the electrostatic charging energy leading to conductance peaks at exact matching. One can observe characteristic peak patterns upon varying: i) the area of the dot by means of a side modulation gate or ii) by tuning the magnetic field (a third possibility not discussed
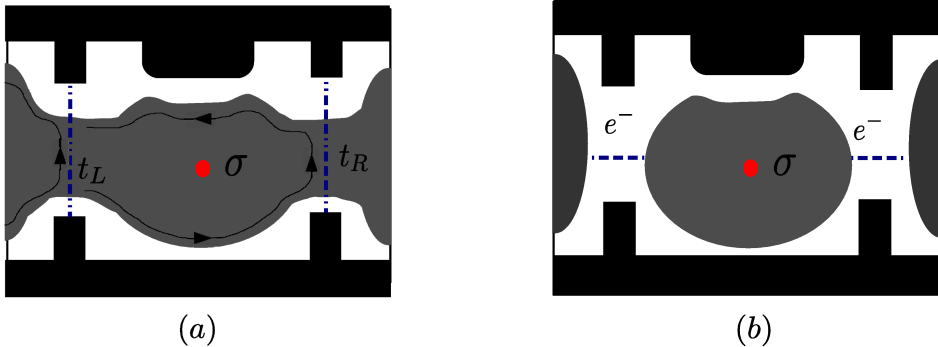
Figure 1: The quantum Hall interferometer: the electron fluid is drawn in the (a) weak and (b) strong backscattering limits.

here could be charging an antidot engineered inside the droplet). The Coulomb blockade in quantum Hall droplets has been considered in [22][23][19], where it was shown to provide interesting tests of the conformal field theory description. Indications of experimental feasibility have been recently reported [24].

In this paper, we obtain the peak patterns from the knowledge of the disk partition function (1.2) [18]. Each $Z_{\text{disk}}^{(\alpha)}$ resums all excitations corresponding to adding electrons to the droplet within the $\alpha$ sector (of given fractional charge): level deformations and degeneracies are all accounted there. We study the peak patterns in the $(S, B)$ plane, corresponding to simultaneous changes of area and magnetic field, and discuss the bulk-edge relaxation (recombination) of neutral excitations.

In section 3, we give a detailed account of the Coulomb blockade in the Jain hierarchical states already presented in [18], as well as the results in two alternative theories for the same states. In section 4, we discuss the case of Read-Rezayi non-Abelian states, extending the results [22][23][19]. The peaks follow a periodic pattern with a modulation in the separations that is due to the presence of neutral excitations. Although the peak patterns are qualitatively similar in the Abelian and non-Abelian cases, there are specific differences:

i) in the Abelian Jain hierarchical case, the energy levels possess multiplicities characteristic of the multicomponent fluids, that can be observed experimentally in the peak patterns; moreover, all features are independent of the bulk quasiparticle sector $\alpha$, and bulk-edge relaxations are not possible.

ii) in the non-Abelian Read-Rezayi states, there are no degeneracies and the peak patterns depend on the sector; furthermore, bulk-edge relaxations could be possible, and would wipe out the dependence on the sector.

In summary, the patterns of Coulomb blockade peaks can test the qualitative properties of the Hilbert space of conformal field theory: the fusion rules, the sectors and the multiplicities of excitations. These features are manifestly shown by the disk partition functions.
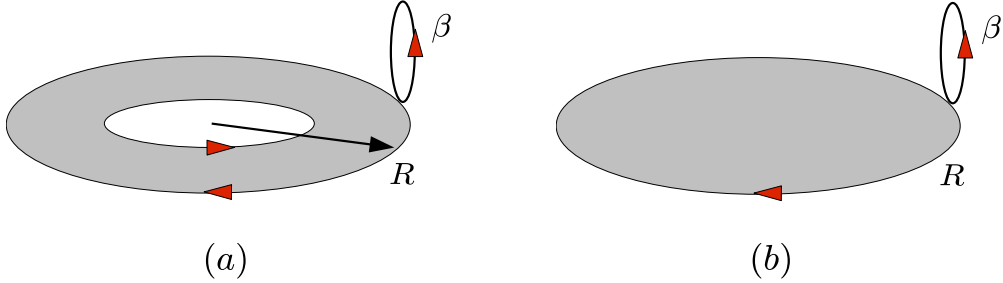
3

Figure 2: The (a) annulus and (b) disk geometries.

# 2 Partition functions in QHE

## 2.1 Annulus geometry

The Hilbert space of a RCFT is made by a finite number of representations of the maximally extended (chiral) symmetry algebra, which contains the Virasoro conformal algebra as a subalgebra [3]. The representations are encoded in the partition function of the Euclidean theory defined on the geometry of a space-time torus $S^1 \times S^1$. Moreover, any RCFT is associated to a Chern-Simons theory, and the torus partition function in the former theory corresponds to a path-integral amplitude for the latter theory on the manifold $S^1 \times S^1 \times \mathbb{R}$, where $\mathbb{R}$ is the time axis [8][25].

In the quantum Hall effect, we can consider a spatial annulus with Euclidean compact time of period $\beta$, the inverse temperature: the topology of this space-time manifold is $\mathcal{M} = S^1 \times S^1 \times I$, where $I$ is the finite interval of the radial coordinate. The partition function of edge excitations is defined on the boundary $\partial \mathcal{M}$, corresponding to two copies of a space-time torus (see Fig. 2(a)). The excitations are chiral and anti-chiral waves on the outer ($R$) and inner ($L$) edges, respectively. The annulus coordinates are $(\varphi, t_E, r)$, with $r \in I = [R_L, R_R]$ and $t_E \equiv t_E + \beta$, $\varphi \equiv \varphi + 2\pi$. We assume that there are no static bulk excitation inside the annulus; they could be added afterwards but will not be necessary.

We illustrate the method and set the notation by first repeating the analysis of the simpler Laughlin states [17]. The following spectrum was obtained for the excitations on each edge from the canonical quantization of the chiral Luttinger liquid [26]:

$$\nu = \frac{1}{p} , \quad Q = \frac{n}{p} , \quad L_0 = \frac{n^2}{2p} , \qquad n \in \mathbb{Z} , \ p = 1, 3, 5, \dots . \tag{2.1}$$

Each pair of values $(Q, L_0)$ are weights of a (highest-weight) representation of the $\widehat{U(1)}$ affine (current) algebra of the conformal theory with central charge $c = 1$, $L_0$ being the zero mode of the Virasoro algebra.

We shall obtain the partition functions $Z_{\text{annulus}}$ by using these data and by imposing

4

the modular invariance conditions. We start by the definition [3]:

$$Z_{\text{annulus}}(\tau, \zeta) \;=\; \mathcal{K} \ \text{Tr} \ \left[ e^{i2\pi\left(\tau\left(L_0^L - c/24\right) - \bar{\tau}\left(L_0^R - c/24\right) + \zeta Q^L + \bar{\zeta} Q^R\right)} \right] \;, \qquad (2.2)$$

where the trace is over the states of the Hilbert space, $\mathcal{K}$ is a normalization to be described later and $(\tau, \zeta)$ are complex numbers. We recognize (2.2) as the grand-canonical partition function: the total Hamiltonian and spin of excitations are:

$$H = \frac{v_R}{R}\left(L_0^R - \frac{c}{24}\right) + \frac{v_L}{R}\left(L_0^L - \frac{c}{24}\right) + V_o\left(Q^L - Q^R\right) + \text{ const.}, \qquad J = L_0^L - L_0^R \;. \tag{2.3}$$

The energy is proportional to the conformal dimension, $E = (v/R)(L_0 - c/24)$, with $c$ parameterizing the Casimir energy [3]. The real and imaginary parts of $(\tau, \zeta)$ are related to the inverse temperature $\beta$ and Fermi velocity $v$, $2\pi R \, \text{Im}\tau = v\beta > 0$, the "torsion" $\text{Re}\tau$, the chemical potential $\mu\beta = 2\pi\text{Re}\zeta$ and the electric potential between the two edges $V_o\beta = 2\pi\text{Im}\zeta$. Since the Virasoro dimension is roughly the square of the charge, the partition sum is convergent for $\text{Im}\tau > 0$ and $\zeta \in \mathbb{C}$. Let us momentarily choose a symmetric Hamiltonian for the two edges by adjusting the velocities of propagation of excitations, $v_L/R_L = v_R/R_R$.

As usual in RCFT, one can divide the trace in (2.2) into a sum over pairs of highest-weight $\widehat{U(1)}$ representations (one for each edge) and then sum over the states within each representation. The latter give rise to the $\widehat{U(1)}$ characters [3]:

$$Ch\left(Q, L_0\right) \;=\; \text{Tr}\big|_{\widehat{U(1)}} \ \left[ e^{i2\pi(\tau(L_0 - c/24) + \zeta Q)} \right] \;=\; \frac{q^{L_0} \, w^Q}{\eta(q)} \;, \qquad (2.4)$$

where $\eta$ is the Dedekind function,

$$\eta(q) = q^{1/24} \prod_{k=1}^{\infty} \left(1 - q^k\right) \;, \qquad q = e^{i2\pi\tau} \;, \quad w = e^{i2\pi\zeta} \;. \qquad (2.5)$$

Any conformal field theory with $c \geq 1$ contains an infinity of Virasoro (and $\widehat{U(1)}$) representations [3]; therefore, we must further regroup the $\widehat{U(1)}$ characters into characters $\theta_\lambda(\tau, \zeta)$ of an extended algebra in order to get the finite-dimensional decomposition:

$$Z_{\text{annulus}} \;=\; \sum_{\lambda, \bar{\lambda}=1}^{N} \mathcal{N}_{\lambda, \mu} \, \theta_\lambda \, \overline{\theta}_\mu^c \;. \qquad (2.6)$$

In this equation, the bar denotes complex conjugation and the suffix $(c)$ is the charge conjugation $C$, acting by: $Q \to -Q$, $\theta \to \theta^c$. The inner (resp. outer) excitations are described by $\theta_\lambda$ (resp. $\theta_\mu^c$), according to the definition (2.2). The coefficients $\mathcal{N}_{\lambda, \mu}$ are positive integers giving the multiplicities of sectors of excitations: they are not known in general, but in cases of explicit path-integral calculations. In the following, we shall self-consistently determine the $\mathcal{N}_{\lambda, \mu}$ by imposing modular invariance and some physical requirements.

## 2.2 Modular invariance conditions

The torus geometry $\mathbb{T}$ can be described as the quotient of the complex plane $\mathbb{C}$ by the lattice of translations $\Lambda$ generated by the two periods $\omega_1$ and $\omega_2$:

$$\mathbb{T} = \frac{\mathbb{C}}{\Lambda} \ , \qquad z \sim z + n_1 \omega_1 + n_2 \omega_2 \ , \qquad z \in \mathbb{C}, \ \ n_1, n_2 \in \mathbb{Z} \ . \tag{2.7}$$

The same lattice can also be generated by another pair of periods $\omega_1'$ and $\omega_2'$, that are related by linear integer transformations with unit determinant, i.e by $SL(2,\mathbb{Z})$ mappings. Owing to scaling invariance, the torus is characterized by the complex modulus, $\tau = \omega_2/\omega_1$, with $\mathrm{Im}\,\tau > 0$. Equivalent coordinates on the torus are related by the modular transformations,

$$\tau' = \frac{a\tau + b}{c\tau + d} \ , \qquad a, b, c, d \in \mathbb{Z} \ , \qquad ad - bc = 1 \ . \tag{2.8}$$

The modular group is thus given by $\Gamma \equiv PSL(2,\mathbb{Z}) = SL(2,\mathbb{Z})/\mathbb{Z}_2$ (the quotient is over the global sign of transformations): it is known that the group has two generators, $T \ : \ \tau \to \tau + 1$ and $S \ : \ \tau \to -1/\tau$, satisfying the relations $S^2 = (ST)^3 = C$, where $C$ is the charge conjugation matrix, $C^2 = 1$ [3] (more details are given in Appendix A).

The invariance of the partition function under modular transformations is therefore given by:

$$Z_{\mathrm{annulus}} \left( \frac{-1}{\tau}, \frac{-\zeta}{\tau} \right) = Z_{\mathrm{annulus}} \left( \tau + 1, \zeta \right) = Z_{\mathrm{annulus}} \left( \tau, \zeta \right) \ . \tag{2.9}$$

Note that the other parameter $\zeta$ transforms under (2.8) as a coordinate on the torus, that acquires the scale factor: $\zeta' = \zeta/(c\tau + d)$.

In the following discussion, these geometrical conditions will be obtained from physical requirements on the QHE system, thus showing that they are appropriate for the CFT description of edge excitations.

The most interesting modular transformation exchanges the two periods of the torus,

$$S : \qquad Z \left( -\frac{1}{\tau}, -\frac{\zeta}{\tau} \right) = Z \left( \tau, \zeta \right) \ . \tag{2.10}$$

From the geometrical standpoint, the equivalence of the periods is apparent in the Chern-Simons theory: the RCFT partition function corresponds to an amplitude on $\mathcal{M} = S^1 \times S^1 \times \mathrm{I}$, where time is $t_E \in \mathrm{I}$ and the two spatial periods are on the same footing [8][25].

From the physical point of view, the $S$ invariance amounts to a completeness condition for the spectrum of the RCFT: upon exchanging time and space, it roughly imposes that the set of states at any time $t_E = t_o$ is the same as that ensuring time

propagation [3]. Furthermore, in RCFT partition functions (2.6), the $S$ transformation is realized by a linear transformation of the characters,

$$\theta_\alpha \left( -\frac{1}{\tau}, -\frac{\zeta}{\tau} \right) = e^{i\varphi} \sum_{\beta=1}^{N} S_{\alpha\beta} \, \theta_\beta \left( \tau, \zeta \right) \, , \qquad (2.11)$$

($\varphi$ is an overall phase to be specified later). Thanks to the Verlinde formula [7], the matrix $S_{\alpha\beta}$ determines the fusion rules of the RCFT that express the consistency and completeness of the operator content of the theory.

Let us remark that the completeness of the operator content can also be enforced by solving the crossing symmetry of 4-point functions, where the fusion rules determine the possible intermediate channels. However, several examples in the literature show that crossing symmetry may be satisfied on smaller set of sectors than those required by the $S$ modular invariance; the latter is a stronger consistency condition requiring "maximal" extension of the operator content [3].

The invariance under the $T$ transformation has the following physical motivation. The partition function should describe physical excitations of the whole sample that can be measured in conduction experiments: these are electron-like and have integer or half-integer spin. Therefore, anyon excitations should pair on the two edges to form them. This condition is enforced by,

$$T^2 : \qquad Z \left( \tau + 2, \zeta \right) \equiv \mathrm{Tr} \, \left[ \cdots \mathrm{e}^{\, i 2\pi \, 2 \left( L_0^L - L_0^R \right)} \right] = Z \left( \tau, \zeta \right) \, . \qquad (2.12)$$

The presence of fermionic states in the QHE implies the weaker modular invariance $T^2$: actually, $S$ and $T^2$ generate a subgroup of the modular group, $\Gamma_\theta \subset \Gamma$, as discussed in appendix A.

The partition function should also be invariant under independent transformations of the coordinate $\zeta$, that express its double periodicity: $\zeta \sim \zeta + 1 \sim \zeta + \tau$. From the physical point of view, these geometrical conditions correspond to requirements on the charge spectrum.

In absence of bulk quasiparticles, the edge excitations should have global integer charge, $Q^L + Q^R \in \mathbb{Z}$, which measures the number of electrons injected into the system by attaching leads to the two edges. This condition reads,

$$U : \qquad Z \left( \tau, \zeta + 1 \right) \equiv \mathrm{Tr} \, \left[ \cdots \mathrm{e}^{\, i 2\pi \left( Q^R + Q^L \right)} \right] = Z \left( \tau, \zeta \right) \, . \qquad (2.13)$$

It follows that fractionally charged excitations at one edge must pair with complementary ones on the other boundary. Consider, for example, $\nu = 1/3$; we can imagine to drop in an electron, which splits into the pair $(Q^L, Q^R) = (1/3, 2/3)$, or into the others, $(0, 1), (2/3, 1/3), (1, 0)$.

The different splittings should all be possible and be equally accounted by the partition function, leading to a further invariance. They are related one to another by tuning the electric potential $V_o$ in (2.3): the change corresponding to adding one

7

flux quantum inside the annulus is, $V_o \to V_o + 1/R$ (in our notations $e = c = \hbar = 1$), and corresponds to $\zeta \to \zeta + \tau$. The invariance of the partition function is therefore,

$$V : \qquad Z(\tau, \zeta + \tau) = Z(\tau, \zeta) \ . \tag{2.14}$$

The transformation of the partition function under $\zeta \to \zeta + \tau$ is called "spectral flow" [26][17][27], for reasons that will be clear momentarily.

We now solve the conditions $(T^2, S, U, V)$ for the $c = 1$ theory. First consider the $U$ condition, $Q^L + Q^R \in \mathbb{Z}$: we collect left $\widehat{U(1)}$ representations which have integer spaced charges, $Q^L = \lambda/p + \mathbb{Z}$, and later combine them with the corresponding right representations. The sums of $\widehat{U(1)}$ characters give theta functions with rational characteristics:

$$
\begin{aligned}
\theta_\lambda &= \mathrm{e}^{-\frac{\pi}{p}\frac{(\mathrm{Im}\zeta)^2}{\mathrm{Im}\tau}} \frac{1}{\eta} K_\lambda(\tau, \zeta; p) \\
&= \mathrm{e}^{-\frac{\pi}{p}\frac{(\mathrm{Im}\zeta)^2}{\mathrm{Im}\tau}} \frac{1}{\eta} \sum_{k \in \mathbb{Z}} \mathrm{e}^{i2\pi \left( \tau \frac{(pk+\lambda)^2}{2p} + \zeta\left(\frac{\lambda}{p} + k\right) \right)} \ ,
\end{aligned}
\tag{2.15}
$$

indeed showing $Q^L = \lambda/p + \mathbb{Z}$, $\lambda = 1, 2, \ldots, p$. (The non-analytic prefactor is explained later). The transformations $T^2, S, U, V$ of these generalized characters are found to be (see Appendix A),

$$
\begin{aligned}
T^2 : \ \theta_\lambda(\tau + 2, \zeta) &= \mathrm{e}^{i2\pi\left(\frac{\lambda^2}{p} - \frac{1}{12}\right)} \theta_\lambda(\tau, \zeta) \ , \\
S : \ \theta_\lambda\left(-\frac{1}{\tau}, -\frac{\zeta}{\tau}\right) &= \frac{\mathrm{e}^{i\frac{\pi}{p}\mathrm{Re}\frac{\zeta^2}{\tau}}}{\sqrt{p}} \sum_{\lambda'=0}^{p-1} \mathrm{e}^{i2\pi\frac{\lambda\lambda'}{p}} \theta_{\lambda'}(\tau, \zeta) \ , \\
U : \ \theta_\lambda(\tau, \zeta + 1) &= \mathrm{e}^{i2\pi\lambda/p} \theta_\lambda(\tau, \zeta) \ , \\
V : \ \theta_\lambda(\tau, \zeta + \tau) &= \mathrm{e}^{-i\frac{2\pi}{p}\left(\mathrm{Re}\zeta + \mathrm{Re}\frac{\tau}{2}\right)} \theta_{\lambda+1}(\tau, \zeta) \ .
\end{aligned}
\tag{2.16}
$$

These transformations show that the generalized characters $\theta_\lambda$ carry a unitary representation of the modular group, which is projective for $\zeta \neq 0$ (the composition law is verified up to a phase).

The corresponding sums of right $\widehat{U(1)}$ representations are given by $\overline{\theta}_\mu^c$ carrying charge $Q^R = \mu/p + \mathbb{Z}$. Finally, the $U$ condition (2.13), applied to $Z_{\text{annulus}}$ (2.6), requires that left and right charges obey: $\lambda + \mu = 0 \mod p$. This form of the partition function also satisfies the other modular conditions, $T^2, S, V$, by unitarity. We finally obtain the modular invariant annulus partition function of Laughlin's plateaus ($c = 1$):

$$Z_{\text{annulus}} = \sum_{\lambda=1}^{p} \theta_\lambda \overline{\theta}_\lambda \ . \tag{2.17}$$

The coefficients, $\mathcal{N}_{\lambda,\mu} = \delta^{(p)}_{\lambda+\mu,0}$, specify the multiplicities and pairings of sectors.

Let us add some remarks on this result.

i) The $U$ condition on the charge spectrum dominates the other ones, because it is linear in the character index $\lambda$: it leads to a unique modular invariant partition function that is left-right diagonal. In other applications of RCFTs, as e.g. in statistical mechanics, the $\zeta$ variable is not usually considered, as well as the corresponding $U, V$ conditions. Therefore, the spectrum of solutions of the remaining conditions, $T, S$, can be rather rich, leading to left-right non-diagonal invariants, such as the ADE classification of $c < 1$ minimal theories [28][3]. In the QHE setting, non-diagonal invariants could possible when neutral sectors of excitations (not constrained by $U$) are included in the theory. Examples for multicomponent Luttinger liquids have been found in [17], but their physical relevance is unclear. In this paper, we shall only consider diagonal modular invariants.

ii) The $V$ transformation illustrates the spectral flow: the addition of a quantum of flux through the center of the annulus is a symmetry of the Hamiltonian but causes a drift of the quantum states among themselves. Indeed, the Hamiltonian (2.3) was made invariant by adding a constant capacitive energy in each sector, $E_c = RV_o^2/2p$, through the non-analytic prefactor in the characters (2.15), $\exp\left(-\nu\pi\left(\text{Im}\zeta\right)^2/\text{Im}\tau\right)$ [17][27]. The modified spectrum of excitations (2.1) is:

$$E_{n_L, n_R} = \frac{v}{R}\frac{1}{2p}\left[(n_L + RV_o)^2 \ + \ (n_R - RV_o)^2\right] \ , \tag{2.18}$$

that has vanishing minimum in both edges for any value of $V_o$. The spectral flow, $\zeta \to \zeta + \tau$, was actually first discussed in Laughlin's thought experiment defining the fractional charge [29][27]. Since the charge transported between the two edges by adding a flux quantum is equal to the Hall conductivity, we find that, $\theta_\lambda(\zeta + \tau) \propto \theta_{\lambda+1}(\zeta)$, does correspond to $\nu = 1/p$. This provides a check of the normalization of $\zeta$.

iii) In the expressions (2.17) one can also verify that all the excitations have integer monodromies with respect to the electrons:

$$J[n_e] + J[n] - J[n_e + n] \in \mathbb{Z} \ , \tag{2.19}$$

where $(n_e = p, n)$ are the integers in (2.1) corresponding to one electron and a generic excitation, respectively.

iv) The generalized characters $\theta_\lambda$ (2.15) correspond to the extension of the $\widehat{U(1)}$ algebra by a chiral current $J_p$. This field is included in the vacuum representation of the extended algebra, and can be identified from the first non-trivial term in the expansion of $\theta_0$ into $\widehat{U(1)}$ characters: $J_p$ has half-integer dimension $L_0 = p/2$ and unit charge. The highest-weight representations of this extended RCFT algebra correspond to generalized primary fields $\phi_\lambda$, whose charge is defined modulo one (the charge of $J_p$); namely, they collect all chiral excitations with the same fractional charge. The fusion rules for these fields are clearly given by the addition of charges modulo $p$,

$$\phi_i \cdot \phi_j \equiv N_{ij}^k \ \phi_k \ , \qquad N_{ij}^k = \delta_{i+j,k}^{(p)} \ , \quad i, j, k \in \mathbb{Z}_p \ , \tag{2.20}$$

that closes on the finite set of $p$ elements.

The same fusion algebra can be obtained by using the Verlinde formula [7],

$$N_{ijk} = \sum_{n=1}^{p} \frac{S_{in}S_{jn}S_{kn}}{S_{0n}} \ . \tag{2.21}$$

Inserting the $S$-modular transformation obtained in (2.16), we find: $N_{ijk} = \delta^{(p)}_{i+j+k,0}$, that is equivalent to (2.20) by lowering one index with the charge-conjugation matrix $C_{ij} = N_{ij0}$ [17].

## 2.3  Disk geometry

From the annulus partition function (2.17), we can deduce the disk partition function by letting the inner radius to vanish, $R_L \to 0$ (see Fig. 2(b)). To this effect, the variable $\bar{\tau}$ in $\bar{\theta}_\lambda$ should be taken independent of $\tau$: $\mathrm{Im}\tau \neq -\mathrm{Im}\bar{\tau}$, $v_R/R_R \neq v_L/R_L$. The annulus partition function is no longer a real positive quantity but remains modular invariant, up to irrelevant global phases. In the limit $R_L \to 0$, the $\bar{\theta}_\lambda$ are dominated by their $|q| \to 0$ behavior: therefore, only the ground state sector remains in (2.17), leading to $\bar{\theta}_\lambda \to \delta_{\lambda,0}$, up to zero-point energy contributions. We find: $Z^{(0)}_{\text{disk}} = \theta_0$. If, however, there are quasiparticles in the bulk with charge, $Q_{\text{Bulk}} = -\alpha/q$, the condition of total integer charge selects another sector, leading to:

$$Z^{(\alpha)}_{\text{disk}} = \theta_\alpha \ . \tag{2.22}$$

Therefore, the disk partition functions are given by the chiral generalized characters $\theta_\alpha$, whose index is selected by the bulk boundary conditions. The set of functions is modular covariant, i.e. it carries a unitary finite-dimensional representation of the modular group, as shown by (2.16).

These partition functions describe the edge physics of isolated Hall droplets with static bulk quasiparticles. Note that each sector has a specific lower-state energy that has been discarded in (2.22): indeed, it is difficult to compare edge energies of different sectors in the disk geometry, because they depend on the external work for adding gapful bulk quasiparticles and other environmental effects [26]. We also remark that the identification of $Z^{(\alpha)}_{\text{disk}}$ from $Z_{\text{annulus}}$ is unique because the sectors relative to the chiral excitations on the outer edge of the annulus (accounted by $\theta_\lambda$) are paired to those of the inner edge ($\bar{\theta}_\lambda$).

# 3  Coulomb blockade in Abelian states

## 3.1  Conductance peaks in Laughlin states

The Coulomb blockade takes place when an electron tunnels in a small quantum dot: the current cannot flow freely because the charging energy may overcame the work

done by the electric potential,

$$\Delta E(n) = -neV + \frac{(ne)^2}{2C} \ , \qquad \Delta Q = -ne \ , \tag{3.1}$$

where $C$ is the capacitance and $V$ the potential. It follows that tunneling is possible when the two terms compensate exactly, $\Delta E(n) = 0$, leading to isolated peaks in the current because the charge is quantized.

In QHE droplet of Fig. 1, the corresponding stationary condition for Coulomb blockade peaks is:

$$E_{S,B}(n+1) = E_{S,B}(n) \ . \tag{3.2}$$

Here, $E_{S,B}(n)$ are the energies for adding $n$ electrons to the edge, that depend on external parameters such as the droplet area $S$ and the magnetic field $B$.

The dependence on area deformations $\Delta S$ can be included in the edge spectrum of Laughlin states (2.1) as follows [23]. The variation of the droplet area induces a deviation of the background charge $Q_{\mathrm{bkg}}$ with respect to its (vanishing) equilibrium value, yielding a contribution to the charge accumulated at the edge, $Q \to (Q - Q_{\mathrm{bkg}})$. The edge energies acquire a electrostatic contribution that can be derived near equilibrium by observing that, $E \propto (Q - Q_{\mathrm{bkg}})^2$. For $\nu = 1/p$, we obtain:

$$E_{\lambda,\sigma}(n) = \frac{v}{R} \frac{(\lambda + pn - \sigma)^2}{2p} \ , \qquad \sigma = \frac{B\Delta S}{\phi_o} \ , \tag{3.3}$$

where $\sigma$ is a dimensionless measure of area deformations.

The Coulomb peaks are obtained by looking for degenerate energy values with $\Delta Q = n$, i.e. within the same fractional charge sector $\lambda$: in Fig. 3(a), we show the dependence of $E_{0,\sigma}(n)$ on $\sigma$: the degeneracy condition (3.2) is satisfied at the midpoints between two consecutive parabolas; there, the electrons can tunnel into the dot yielding the conductance peaks. The separation between two consecutive peaks is:

$$\Delta \sigma = p = \frac{1}{\nu} \ , \qquad \Delta S = \frac{e}{n_o} \ . \tag{3.4}$$

This result is consistent with the classical picture for which the change in the area precisely matches the value required for incorporating one electron at the average density $n_o$ [22].

We now reobtain the conductance peaks from the analysis of the disk partition function, illustrating the method that will be extensively used in the following sections. The disk partition function for $\nu = 1/p$ (2.22) including the area deformation reads, up to irrelevant factors:

$$\theta_\lambda = K_\lambda(\tau, \zeta; p) = \frac{1}{\eta} \sum_{n=-\infty}^{\infty} \exp\left[ i2\pi \left( \tau \frac{(np + \lambda - \sigma)^2}{2p} + \zeta \frac{np + \lambda}{p} \right) \right] . \tag{3.5}$$

Consider the Hall droplet without quasiparticles in the bulk corresponding to $\lambda = 0$: from the character $K_0$ (3.5), we can extract the energies and charges of the electron
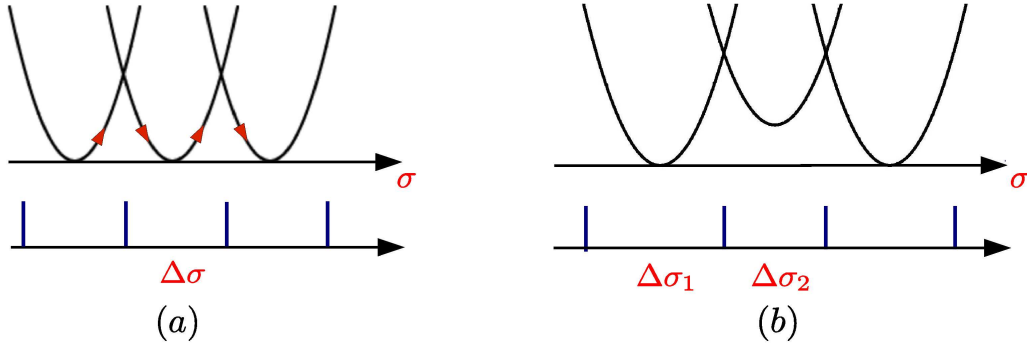
11

Figure 3: Energy levels as a function of the area deformation $\Delta\sigma$: (a) Laughlin states and (b) $m = 2$ Jain hierarchical states.

excitations as the factors multiplying $\tau$ and $\zeta$, respectively. Upon deformation of the dot area, the ground state energy, $E \sim \sigma^2/2p$, $Q = 0$, and that of the one-electron state, $E \sim (\sigma - p)^2/2p$, $Q = 1$, become degenerate at the midpoint $\sigma = p/2$, leading again to (3.4). In the presence of quasiparticles in the bulk with charge $Q = -\alpha/p$, one should repeat the analysis using the partition functions $\theta_\alpha$ (2.22): one obtains the same peak separations, because the energies in the different $\lambda$ sectors are related by global shifts of $\sigma$.

We see that the disk partition function is rather convenient for studying the Coulomb blockade: its decomposition into sectors clearly indicates the allowed electron transitions and considerably simplifies the analysis of more involved theories of the following sections. The strategy will be to first obtain the modular invariant $Z_{\mathrm{annulus}}$ and then analyze the deformed energy spectra within each disk sector.

We now discuss the peaks for variations of the magnetic field $\Delta B$. The chiral Luttinger RCFT is sensitive to flux changes, $\delta = \Delta\phi/\phi_o = S\Delta B/\phi_o$, as follows [17]: the partition functions are deformed by $K_\lambda \rightarrow K_{\lambda+\delta}$, in (3.5) with $\sigma = 0$ , i.e. the energies and charges of all states are changed. For one quantum of flux, $\delta = 1$, each $\lambda$-sector ($\theta_\lambda$) goes into the following one: this is the spectral flow discussed in the previous section. For example, the ground state $\theta_0$ becomes the one-anyon sector $\theta_1$, meaning that the higher $B$ has induced a quasi-hole of charge $-1/q$ in the bulk and the edge states have adjusted correspondingly [27].

As a matter of fact, the dependence of conductance peaks on variations of $B$ is the same as that for variations of $S$, because the edge energies depend of the combined variable $(\delta - \sigma)$,

$$E_{\lambda,\sigma,\delta}(n) = \frac{v}{R}\frac{(\lambda + pn + \delta - \sigma)^2}{2p} \ . \tag{3.6}$$

It is nevertheless important to stress the difference between $S$ and $B$ deformations: the former is a nonrelativistic electrostatic effect, causing no change in the quantization of the Luttinger liquid theory. The latter is the relativistic effect of the chiral anomaly, leading to charge nonconservation at the edge and the spectral flow [26].

12

## 3.2 Partition functions of hierarchical states

The multi-component generalization of the Abelian theory of the previous section is obtained as follows [10]: the electron fluid is assumed to have $m$ independent edges, each one described by a Luttinger liquid, altogether yielding the $\widehat{U(1)}^{\otimes m}$ affine algebra [3]. Its representations are labeled by a vector of (mathematical) charges $r_a, a = 1, \ldots, m$, which spans an $m$-dimensional lattice, $\vec{r} = \sum_i \vec{v}^{(i)} n_i$, $n_i \in \mathbb{Z}$, that is the closed set for the addition of charge vectors (the Abelian fusion rules). The physical charge is a linear functional of $\vec{r}$ and the Virasoro dimension is a quadratic form, both parameterized by the metric of the lattice, $K_{ij}^{-1} = \vec{v}^{(i)} \cdot \vec{v}^{(j)}$. The spectrum is therefore:

$$
\begin{aligned}
Q &= \sum_{i,j=1}^{m} t_i \, K_{ij}^{-1} \, n_j \,, \qquad n_i \in \mathbb{Z} \,, \\
L_0 &= \frac{1}{2} \sum_{i,j=1}^{m} n_i \, K_{ij}^{-1} \, n_j \,, \\
\nu &= \sum_{i,j=1}^{m} t_i \, K_{ij}^{-1} \, t_j \,.
\end{aligned}
\tag{3.7}
$$

In these expressions, $K$ is an arbitrary symmetric matrix of couplings, with integer elements, odd on the diagonal, due to requirement that the spectrum contains $m$ electron-like excitations [10]. The vector $\vec{t}$ can be set to, $\vec{t} = (1, \ldots, 1)$, in a standard basis [10]. The spectrum (3.7) is very general due to the many free parameters in the $K$ matrix: these can actually be chosen to reproduce the results of all known hierarchical constructions of wave functions [1].

The prominent Jain hierarchical states [15], with filling fraction $\nu = m/(ms \pm 1)$, $m = 2, 3, \ldots$, $s = 2, 4, \ldots$, where shown to correspond to the matrices $K_{ij} = \pm \delta_{ij} + s \, P_{ij}$, where $s > 0$ is an even integer and $P_{ij} = 1$, $\forall \, i, j = 1, \ldots, m$ [10]. The Jain spectrum is:

$$
\begin{aligned}
\nu &= \frac{m}{ms \pm 1} \,, \qquad s > 0 \text{ even integer} \,, \qquad c = m \,, \\
Q &= \frac{1}{ms \pm 1} \sum_{i=1}^{m} n_i \,, \\
L_0 &= \pm \frac{1}{2} \left( \sum_{i=1}^{m} n_i^2 - \frac{s}{ms \pm 1} \left( \sum_{i=1}^{m} n_i \right)^2 \right) \,.
\end{aligned}
\tag{3.8}
$$

(Let us first disregard the case with the minus signs, corresponding to antichiral neutral excitations). The spectrum (3.8) is rather peculiar because it contains $m(m-1)$ *neutral* states with unit Virasoro dimension, $(Q, L_0) = (0, 1)$. By using a bosonic free field construction, one can show that these are chiral currents $J_{\vec{\beta}}$, that can be labeled by the simple roots of $SU(m)$ and generate the $\widehat{U(1)} \otimes \widehat{SU(m)}_1$ affine algebra at level one $(c = m)$ [10][13].

The annulus partition functions for multicomponent Luttinger liquids were obtained in [17]: we recall their expressions, first for general $K$-matrix theories and then for the Jain hierarchy.

As in the previous section, the $U$ modular condition is the most relevant one. In order to solve it, we first group the states with integer-spaced charges in the $K$ lattice (3.7). These are clearly parameterized by $\vec{n} = K\vec{\ell} + \vec{\lambda}$ , with $\vec{\ell} \in \mathbb{Z}^m$. Since $K$ is an integer matrix, there is a finite number of $\vec{\lambda}$ values (the sectors of the RCFT), belonging to the quotient of the $\vec{n}$ lattice by the $\vec{\ell}$ lattice:

$$\vec{\lambda} \in \frac{\mathbb{Z}^m}{K\,\mathbb{Z}^m} \ . \tag{3.9}$$

As in section 2.2, the $\widehat{U(1)}$ characters in each sector sum up into $m$-dimensional generalization of the theta functions (2.15):

$$\theta_{\vec{\lambda}} = \mathrm{e}^{-\pi\, t^T K^{-1} t\, \frac{(\mathrm{Im}\zeta)^2}{\mathrm{Im}\tau}} \times$$
$$\frac{1}{\eta(q)^m} \sum_{\vec{\ell}\,\in\,\mathbb{Z}^m} \mathrm{e}^{i2\pi \left[ \frac{\tau}{2} \left( K\vec{\ell} + \vec{\lambda} \right)^T K^{-1} \left( K\vec{\ell} + \vec{\lambda} \right) + \zeta\, \vec{t}^T \left( \vec{\ell} + K^{-1}\vec{\lambda} \right) \right]} \tag{3.10}$$

Their $T^2, S, U, V$ transformations are straightforward generalizations of (2.16) and can be found in [17]: again, the characters (3.10) carry a finite-dimensional unitary projective representation of the modular group. The dimension of representation is $|\det K|$ from (3.9) and matches the Wen topological order.

The $U$ invariance of the annulus partition function, written as a sesquilinear form of the characters (3.10), implies the equation $t^T K^{-1}(\vec{\lambda} + \vec{\mu}) \in \mathbb{Z}$ for the left and right weights. Its solutions depend on the specific form of $K$; here, we shall only discuss the diagonal solution, $\vec{\lambda} + \vec{\mu} = 0$, that also solves the other $(T^2, S, V)$ conditions. Therefore, the modular invariant partition function is:

$$Z_{\mathrm{annulus}}^{\widehat{U(1)}^{\otimes m}} = \sum_{\vec{\lambda} \in \mathbb{Z}^m / K\mathbb{Z}^m} \theta_{\vec{\lambda}}\, \overline{\theta}_{\vec{\lambda}} \ . \tag{3.11}$$

In the Jain hierarchical case, the $\widehat{SU(m)}_1$ symmetry can be used to rewrite sums of $(m-1)$-dimensional $\widehat{U(1)}$ characters into generalized characters pertaining to representations of this extended symmetry: indeed, all states in the $(m-1)$-dimensional sectors have integer-spaced dimensions. The $\widehat{SU(m)}_1$ representations and characters were described in Ref.[30]: there are $m$ highest weight representations, corresponding to completely antisymmetric tensor representations of the $SU(m)$ Lie algebra. They are characterized by an additive quantum number modulo $m$, the so-called $m$-ality, $\alpha = 1, \ldots, m$: thus, the $\widehat{SU(m)}_1$ fusion rules are isomorphic to the $\mathbb{Z}_m$ group. Since the $\widehat{SU(m)}_1$ excitations are neutral, we shall need their characters for $\zeta = 0$, denoted

by $\chi_\alpha(\tau, 0)$: they clearly obey $\chi_\alpha(\tau, 0) = \chi_{\alpha \pm m}(\tau, 0)$. The Virasoro dimension of $\widehat{SU(m)}_1$ representations is:

$$h_\alpha = \frac{\alpha(m - \alpha)}{2m} , \qquad \alpha = 0, \ldots, m - 1 , \tag{3.12}$$

The explicit form of the $\widehat{SU(m)}_1$ characters will not be necessary in the following, but their leading $|q| \to 0$ behavior:

$$\chi_\alpha(\tau) \sim \binom{m}{\alpha} \exp\left[ i2\pi\tau \frac{v_n}{v} \left( \frac{\alpha(m - \alpha)}{2m} - \frac{m - 1}{24} \right) \right] + \cdots, \qquad \alpha = 0, 1, \ldots, m - 1 . \tag{3.13}$$

In this expression we introduced a different Fermi velocity $v_n$ for neutral edge excitations, whose experimental value is expected to be, $v_n \sim v/10$ [22].

The modular transformations of $\widehat{SU(m)}_1$ characters are [30],

$$T^2 : \chi_\alpha(\tau + 2) = e^{i2\pi\left( \frac{\alpha(m - \alpha)}{m} - \frac{m - 1}{12} \right)} \chi_\alpha(\tau) ,$$

$$S : \chi_\alpha\left(-\frac{1}{\tau}\right) = \frac{1}{\sqrt{m}} \sum_{\alpha'=1}^m e^{-i2\pi\frac{\alpha\alpha'}{m}} \chi_{\alpha'}(\tau) , \tag{3.14}$$

while $U, V$ do not act on neutral states.

Furthermore, the $\widehat{U(1)}$ states in $\widehat{U(1)} \otimes \widehat{SU(m)}_1$ theories can be described by the $\mathbb{Z}_p$ characters (2.15) of section 2.2, with free parameter $p$, $K_\lambda(\tau, \zeta; p)$, with $\lambda = 1, \ldots, p$. In summary, the modular invariance problem can be reformulated in the two-dimensional basis of $K_\lambda \chi_\alpha$ characters. The derivation of the partition functions in this basis [17] is rather instructive for the analysis of Read-Rezayi states of the next section.

The Jain spectrum (3.8) can be rewritten in a basis that makes apparent the decomposition into $\widehat{U(1)}$ and $\widehat{SU(m)}_1$ sectors: upon substitution of,

$$n_1 = l + \sum_{i=2}^m k_i \pm \alpha , \qquad n_i = l - k_i , \ i = 2, \ldots, m , \tag{3.15}$$

where $l, k_i \in \mathbb{Z}$ and $\alpha$ is the $\widehat{SU(m)}_1$ weight, we find:

$$\nu = \frac{m}{ms \pm 1} , \qquad Q = \frac{ml \pm \alpha}{ms \pm 1} ,$$

$$L_0 = \frac{(ml \pm \alpha)^2}{2m(ms \pm 1)} \pm \frac{\alpha(m - \alpha)}{2m} + r , \quad r \in \mathbb{Z} . \tag{3.16}$$

Consider these formulas with the upper signs, the other choice will be discussed later. One recognizes the $\widehat{SU(m)}_1$ contributions to $L_0$ (3.12), while the $\widehat{U(1)}$ part identifies

15

the parameters of $K_\lambda$ as $p = m\hat{p}$, $\hat{p} = (ms+1)$ and $\lambda = ml + \alpha \mod (m\hat{p})$; note that $\hat{p} = 1 \mod m$ and $\lambda = \alpha \mod m$, and that $\hat{p}, m$ are coprime numbers $(\hat{p}, m) = 1$. The normalization of $\zeta$ is chosen for $K_\lambda$ (2.15) to reproduce the spectrum (3.16): this is, $K_\lambda(\tau, m\zeta; p)$.

The tensor characters $K_\lambda \chi_\alpha$ form a $(m^2 \hat{p})$ dimensional basis on which the $S$ transformation act as the $\mathbb{Z}_{m\hat{p}} \times \mathbb{Z}_m$ Fourier transform. The analysis of the spectrum shows that charged and neutral excitations are paired by the condition $\lambda = \alpha \mod m$: therefore, we should choose a subspace of tensor characters that obeys this condition and is closed under modular transformations. The dimension of this subspace is the topological order $\hat{p}$. A well-known trick to reduce the space of the discrete Fourier transform by a a square factor $m^2$ [28] is to consider the following $m$-term linear combinations of characters obeying $\lambda = \alpha \mod m$ [17],

$$\mathrm{Ch}_\lambda(\tau, \zeta) = \sum_{\beta=1}^{m} K_{\lambda+\beta\hat{p}}(\tau, m\zeta; m\hat{p}) \ \chi_{\lambda+\beta\hat{p} \mod m}(\tau, 0) \ , \qquad \lambda = 1, \ldots, m\hat{p} \ . \quad (3.17)$$

These characters satisfy $\mathrm{Ch}_{\lambda+\hat{p}} = \mathrm{Ch}_\lambda$; thus, there are $\hat{p}$ independent ones, which can be chosen to be (due to $\hat{p} = 1 \mod m$):

$$\theta_a = \mathrm{Ch}_{ma} \ , \qquad a = 1, \ldots, \hat{p} \ , \qquad \hat{p} = ms + 1 \ . \quad (3.18)$$

One can check that these generalized characters $\theta_a$ carry a $\hat{p}$ dimensional representation of the modular transformations $(T^2, S, U, V)$, with $S_{ab} \propto \exp(i2\pi \ mab/\hat{p})/\sqrt{\hat{p}}$. The modular invariant annulus partition function is therefore the diagonal expression in these characters:

$$Z_{\mathrm{annulus}}^{\widehat{U(1)} \times \widehat{SU(m)}_1} = \sum_{a=1}^{\hat{p}} \theta_a \ \bar{\theta}_a = \sum_{a=1}^{\hat{p}} \left( \sum_{\alpha=1}^{m} K_{ma+\alpha\hat{p}} \ \chi_\alpha \right) \left( \sum_{\beta=1}^{m} \overline{K}_{ma+\beta\hat{p}} \ \overline{\chi}_\beta \right) \ . \quad (3.19)$$

Indeed, the characters $\theta_a$ can be shown to be equal to the $\chi_{\vec{\lambda}}$ in (3.10) for $K = 1 + sC$, once the corresponding $\widehat{U(1)}$ charges are identified [17].

The $V$ transformation,

$$V \ : \ \theta_a(\tau, \zeta+1) = \mathrm{e}^{-i2\pi \frac{m}{\hat{p}} \left( \mathrm{Re}\zeta + \mathrm{Re}\frac{\tau}{2} \right)} \theta_{a+1}(\tau, \zeta) \ , \quad (3.20)$$

shows that the minimal transport of charge between the two edges is $m$ times the elementary fractional charge; this is the smallest spectral flow among the states contained in (3.17) which keeps $\beta$ constant, namely which conserves the $\widehat{SU(m)}_1$ quantum number carried by the neutral excitations. The Hall current, $\nu = m/\hat{p}$, is thus recovered.

We now give the partition functions for Jain states with charged and neutral excitations of opposite chiralities on each edge, corresponding to $\nu = m/(ms-1)$ in (3.8)

[17]. The chirality of the neutral excitations can be switched by a simple modification of the characters (3.17),

$$\mathrm{Ch}_\lambda^{(-)} = \sum_{\beta=1}^m K_{\lambda+\alpha\hat{p}}\left(\tau, m\zeta; m\hat{p}\right) \ \overline{\chi}_{\lambda+\beta\hat{p} \ \mathrm{mod} \ m} \ , \qquad \lambda = 1, \ldots, m\hat{p} = m(ms-1) \ .$$

(3.21)

This gives again a representation of the modular group for $\hat{p} = ms - 1 > 0$. The $U$ condition implies the partition function:

$$Z_{\mathrm{annulus}}^{(-)} = \sum_{a=1}^{\hat{p}} \left( \sum_{\alpha=1}^m K_{ma+\alpha\hat{p}} \ \overline{\chi}_\alpha \right) \left( \sum_{\beta=1}^m \overline{K}_{ma+\beta\hat{p}} \ \chi_\beta \right) \ .$$

(3.22)

that is modular invariant and reproduces the spectrum (3.8) for $\nu = m/(ms-1)$.

## 3.3  Coulomb peaks in hierarchical states

The following disk partition functions can be extracted from the annulus expressions (3.19),

$$Z_{\mathrm{disk},a}^{\widehat{U(1)}\otimes\widehat{SU(m)}_1} = \theta_a = \sum_{\beta=1}^m K_{ma+\beta\hat{p}}(\tau, m\zeta; m\hat{p}) \ \chi_\beta(\tau) \ , \quad a = 1, \ldots, \hat{p},$$

(3.23)

where $\hat{p} = ms + 1$. The novelty w.r.t. the Laughlin case of section 3.1, is that each sector contains combined charged and neutral excitations, that are described by the $K_\lambda$ (3.5) and $\chi_\alpha(\tau)$ (3.13) characters, respectively. For example, in the $\nu = 2/5$ case, $(m = 2, \hat{p} = 5)$, there are two neutral characters that combine with ten charged ones to obtain the following five sectors:

$$\begin{aligned}
\theta_0 &= K_0(\tau, 2\zeta; 10) \ \chi_0 + K_5(\tau, 2\zeta; 10) \ \chi_1 \ , \\
\theta_{\pm 1} &= K_{\pm 2}(\tau, 2\zeta; 10) \ \chi_0 + K_{5\pm 2}(\tau, 2\zeta; 10) \ \chi_1 \ , \\
\theta_{\pm 2} &= K_{\pm 4}(\tau, 2\zeta; 10) \ \chi_0 + K_{5\pm 4}(\tau, 2\zeta; 10) \ \chi_1 \ .
\end{aligned}$$

(3.24)

We now search for degeneracy of energy levels differing by the addition of one electron, $\Delta Q = 1$. Consider for definiteness the $\nu = 2/5$ case without any bulk quasiparticle, i.e. $\theta_0$ above. From the expressions (3.5, 3.23, 3.24), one finds that the first term $K_0$ resumes all even integer charged excitations, while $K_5$ the odd integer ones. Therefore, the first conductance peak is found when the lowest energy state in $K_0 \ \chi_0$, i.e. the ground state, with $E = (v_c/R)(2\sigma)^2/20$, $Q = 0$, becomes degenerate with the lowest one in $K_5 \ \chi_1$, with $E = (v_c/R)(-5 + 2\sigma)^2/20 + v_n/4R$, $Q = 1$. The next peak occurs when the latter becomes degenerate with the first excited state ($Q = 2$) in $K_0 \ \chi_0$, and so on. Owing to the contribution of the neutral energy in $\chi_1$ (cf. (3.13)), the level matching is not midway and there is a bunching of peaks in pairs, with separations $\sigma = 5/2 \mp v_n/2v$ (see Fig. 3(b)). Note that in the previous energies we modified $\sigma \to 2\sigma$, (cf. (3.5)), in order to respect the flux-charge relation, $\Delta Q = \nu \Delta\phi/\phi_o$.

For general $m$ values, the result can be similarly obtained by comparing the energies in consecutive pairs of terms, $\beta$ and $\beta+1$, in $\theta_0$ (3.23). One finds:

$$\Delta\sigma_\beta = \sigma_{\beta+1} - \sigma_\beta = \frac{\hat{p}}{m} + \frac{v_n}{v}\left(h_{\beta+2} - 2h_{\beta+1} + h_\beta\right) . \qquad (3.25)$$

where $h_\beta$ are the $\widehat{SU(m)}_1$ dimensions (3.12). Since they are quadratic in $\beta$, the discrete second derivative in (3.25) is constant, except for one value at the border of the $m$ period. This implies that there are groups of $m$ equally spaced peaks, with a larger spacing between groups.

An important fact shown by the $\widehat{SU(m)}_1$ character (3.13), is that the low-lying neutral states occur with characteristic multiplicities $d_\beta = \binom{m}{\beta}$. This means that $d_\beta$ degenerate states are simultaneously made available for the $\beta$-th electron to tunnel into the droplet. These multiplicities can be easily understood in a classical model of $m$ superposed fluids, where the one-electron excitation is $m$ times degenerate, the two-electron one is $m(m-1)/2$ times and so on.

Summarizing, in the Jain hierarchical states, $\nu = m/\hat{p}$, the peak pattern is the following: the separation $\Delta\sigma_k$ between the $k$-th and $(k+1)$-th peaks and the level multiplicity $d_k$ read ($\sigma = B\Delta S/\phi_o$):

$$\begin{aligned}
\Delta\sigma_k &= \frac{\hat{p}}{m} - \frac{v_n}{v}\frac{1}{m} , & d_k &= \binom{m}{k} , \quad k = 1, \ldots, m-1, \\
\Delta\sigma_m &= \frac{\hat{p}}{m} + \frac{v_n}{v}\frac{m-1}{m} , & d_m &= 1 .
\end{aligned} \qquad (3.26)$$

The pattern repeats with periodicity $m$. It is independent of the presence of quasiparticles in the bulk, because the corresponding sectors, $\theta_a$, $a \neq 0$, have linearly shifted energies w.r.t those of $\theta_0$ (cf.(3.23)) [18]. Note that the bulk quasiparticles have the same multiplicities: for example, at $\nu = 2/5$ there are two quasiparticles with $Q = 1/5$ (cf. (3.24)). In presence of quasiparticles with multiplicity $\binom{m}{k-1}$, the sequence of peaks (3.26) starts from $\Delta\sigma_k$ (instead of $\Delta\sigma_1$) and goes on periodically. We remark that the results (3.26) can also be obtained from the analysis of the $m$-dimensional lattice of excitations (3.8), where the multiplicities $d_k$ are found by counting the shortest vectors with integer charge $k$.

The multiplicities $d_\beta$ of low-lying edge excitations could be experimentally observed in the Coulomb peaks as follows. We expect that the degeneracy is broken by finite-size effects, such as perturbations of the CFT by irrelevant operators, that could be non-negligible for small droplets, with sizes of the order of one micron, where Coulomb blockade effects are expected to be found [24]. (Further level splittings could arise for unequal values of the $(m-1)$ neutral modes velocities.) If the symmetry breaking is small, the levels have a fine structure and the electrons tunneling into them yield peaks at different, slightly displaced distances: upon superposing several periods of Coulomb peaks, one can observe the patterns shown in Fig. 4 for $m = 3, 4$. The single peak at the end of the periods can be taken as a reference point for the superpositions and as a measure of experimental errors.
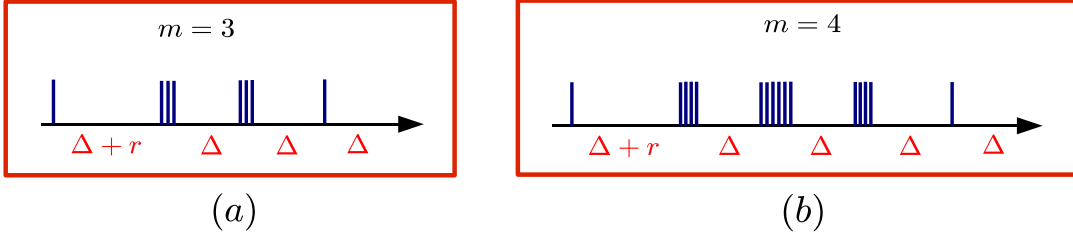
Figure 4: Coulomb peaks in $m = 3$ and $m = 4$ Jain hierarchical states; the extra separation is $r = v_n/v \sim 0.1$.

In conclusion, the multiplicities of Jain hierarchical fluids are observable if the experimental precision is sufficiently high and the $\widehat{SU(m)}_1$ symmetry is not strongly broken. Note that decays among the fine-structured levels are possible and could take place on short time scales; higher levels in the multiplets are nevertheless populated due to thermal fluctuations. (Earlier discussions [18] of experimental signatures of level multiplicities were not completely correct).

We now consider the Jain hierarchical states with mixed chiralities, $\nu = m/(ms-1)$, described by the disk partition functions (3.21). These were obtained by the replacement, $\chi_\beta \to \overline{\chi}_\beta$, that does not affect the earlier discussion of energetics. Therefore, the formulae (3.26) also hold in these cases, upon replacing $\hat{p} = ms - 1$, and predict the same peak multiplicities.

The dynamics of these $m$-composite edge theories was much discussed in the literature, starting from the experimental result [31]. Actually, the presence for $\nu = m/(ms - 1)$ of neutral and charged excitations of opposite chiralities on the same edge may allow for destabilizing interactions, leading to edge reconstruction effects [32]. Several deformations of, or additions to the Luttinger liquid Hamiltonian, have been put forward; as these break the $\widehat{SU(m)}_1$ symmetry and possibly the conformal symmetry, they may lift the peak degeneracy. Therefore, it is interesting to find their predictions for the Coulomb peak patterns and compare with the present results of the $m$-component Abelian theory.

## 3.4 Coulomb peaks in alternative hierarchical theories

In this subsection we discuss the Coulomb peaks in two alternative theories of the Jain states: the $W_{1+\infty}$ minimal models [13], introduced by Trugenberger and some of the authors, and the three-fluid theory [14] by Fradkin and Lopez. Both theories:

i) possess a reduced number of currents and more generally less degrees of freedom w.r.t. the $m$ component Luttinger theory;

ii) are not rational CFT, i.e. their partition function are not modular invariant. Nevertheless, these theories are projections of RCFTs and the partition function can be found by working out the reduction of degrees of freedom; the Coulomb blockade

19

peaks are then found by the same methods as before.

We first discuss the minimal $W_{1+\infty}$ models [13]: these theories were introduced by exploiting the main geometrical feature of incompressible Hall fluids, which is the symmetry under area-preserving diffeomorphisms of the plane, the local coordinate transformations that keep the density constant [33]. The edge excitations can be seen as infinitesimal area-preserving deformations of the Hall droplet , and can be naturally described by the representations of the symmetry algebra. In the mathematical literature, this is called the $W_{1+\infty}$ algebra and its representations on the circle, i.e. on the edge CFT, have been completely classified [34].

The mathematical results are the following: for generic parameters, the $W_{1+\infty}$ representations are isomorphic to those of the multicomponent Luttinger theory and their $m$ dimensional $K$ lattices. However, for special lattices, there exist degenerate representations, with a reduced set of excitations: as shown in [13], these correspond one-to-one with the $\widehat{SU(m)}_1$ symmetric lattices of the Jain states discussed before. For these theories, it is thus possible to project out states of the Luttinger theory and obtain the minimal $W_{1+\infty}$ models made of irreducible representations only. The main features of these models are [13]:

i) the multiplicities due to the $SU(m)$ symmetry are completely eliminated; in particular, there is only one conserved $U(1)$ current, the electric current, a single electron state (not $m$) and no further degeneracies in the spectrum. The charges and conformal dimensions are still given by the formulas (3.8), but the integer labels are constrained within the wedge,

$$n_1 \geq n_2 \geq \ldots \geq n_m \; ; \tag{3.27}$$

ii) the conformal symmetry is maintained, but the partition function is not modular invariant. The projection from the $m$ component Luttinger liquid to the minimal models can be realized by introducing a non-local, $\widehat{SU(m)}_1$ breaking interaction in the Luttinger Hamiltonian, that commutes with Virasoro [35]. This term is diagonal in the $SU(m)$ basis and gives higher energies to the unwanted states; at infinite coupling the projection is realized leading to the $W_{1+\infty}$ minimal theory. The non-locality of the interaction term in the Hamiltonian explains the lack of modular invariance in these theories.

The conductance peaks in the minimal $W_{1+\infty}$ theories are easily obtained: since the projection preserves the structure of the Hilbert space of the $(c = m)$ Luttinger theory, it does not modify the structure of disk partition functions (3.23), but only replaces the neutral characters $\chi_\alpha$ by other expressions whose leading terms (3.13) have no multiplicity factors [36]:

$$\chi_\alpha^{W_{1+\infty}}(\tau) \sim \exp\left[i2\pi\tau\frac{v_n}{v}\left(\frac{\alpha(m-\alpha)}{2m} - \frac{m-1}{24}\right)\right] + \cdots, \qquad \alpha = 0, 1, \ldots, m-1 \; . \tag{3.28}$$

The absence of multiplicities can also be understood from the charge lattice (3.8) as due to the constraint (3.27). We conclude that the $W_{1+\infty}$ minimal models predict

20

conductance peaks in Jain states with the same pattern (3.26) as the Luttinger theory but without any multiplicity.

The Lopez-Fradkin theory of Jain's states is a variant of the multicomponent Luttinger liquid and can be formulated in the charge lattice approach introduced before: all Jain states, $\nu = m/(ms+1)$, $s$ even, are described by the same three-dimensional $K$ matrix and charge vector $t$,

$$K = \begin{pmatrix} -s & 1 & o \\ 1 & m & 0 \\ 0 & 0 & 1 \end{pmatrix} , \qquad t = (1, 0, 0) . \tag{3.29}$$

The first component clearly describes the charged excitations; the other two sectors are called topological, because their neutral excitations do not propagate, i.e. $v_n = 0$. This choice modifies the time scaling of the electron correlator: for $1/3 < \nu < 1/2$, the multicomponent Luttinger theory predicts a constant exponent $\alpha = 3$, while the Lopez-Fradkin theory a varying one, $\alpha = 1/\nu$, which is in better agreement with the experimental results [31]. Note, however, that the $m$ component Luttinger theory also predicts $\alpha = 1/\nu$ in the limit $v_n = 0$, while other experiments would favor $0 < v_n \ll v$ [37].

Another feature of Lopez-Fradkin theory is that the excitations are described by a subspace of the three dimensional charge lattice (3.7): the integers $(n_1, n_2, n_3)$ labeling excitations are constrained by the condition of physical states, $n_2 = -n_3$. Therefore, the partition function has the general charge-lattice form (3.11), but it is not modular invariant due to this constraint.

The Coulomb peaks in this theory are equidistant because the modulations are proportional to $v_n/v = 0$: moreover, there is a single electron excitation and no level multiplicities because the two dimensional sublattice of (3.29) has no symmetries. For the same reason, the Coulomb peaks would be equally spaced even for $v_n > 0$.

In conclusion, we have shown that three proposed theories for the Jain states predict rather different patterns of conductance peaks that would be interesting to test experimentally. Other edge theories have been proposed whose peak patters remain to be investigated [32].

# 4    Coulomb Blockade in Read-Rezayi states

The Pfaffian ($k = 2$) [38] and Read-Rezayi ($k = 3, 4, \ldots$) [11] theories are prominent candidates for describing spin-polarized Hall plateaux observed in the second Landau level [39]. The wave functions of these theories describe electrons that first bound themselves into $k$-clusters and then form incompressible fluids. In particular, the $k = 2$ state corresponds to a two-dimensional p-wave superconductor [40] and should be realized at $\nu = 5/2$. These states are the present best candidates for observing excitations with non-Abelian statistics [4] and for manipulating them to

21

realize the unitary transformations of quantum computation, following the proposal of topological quantum computation [5]. Therefore, Coulomb blockade and interferometry of edge excitations are actively investigated in these states both theoretically and experimentally [22][23][19][24].

The filling fractions are:

$$\nu = 2 + \frac{k}{kM + 2} \ , \qquad k = 2, 3, \ldots, \quad M = 1, 3, \ldots \tag{4.1}$$

The RCFT description is based on a charged Luttinger field and the neutral $\mathbb{Z}_k$ parafermion theory, $\widehat{U(1)} \times \mathrm{PF}_k$, with central charge $c = 1 + \frac{2(k-1)}{k+2}$ [12]. The best observable plateaus correspond to $M = 1$ but we shall provide formulas for the general case. From the wave function constructions and earlier analyses, the following spectrum has been found [20]:

$$\begin{aligned}
Q &= \frac{m}{kM + 2} + s \ , \quad s \in \mathbb{Z} \ , \\
L_0 &= \frac{(m + s(kM + 2))^2}{2k(kM + 2)} + h_m^\ell \ ,
\end{aligned} \tag{4.2}$$

where $h_m^\ell$ is the dimension of parafermion states to be described momentarily. The topological order, i.e. the number of sectors of the RCFT, is:

$$\frac{(k + 1)(kM + 2)}{2} \ , \tag{4.3}$$

and is obtained as follows. The fractional charge, $Q = \lambda/(kM + 2)$, implies $(kM + 2)$ Abelian sectors, and the $\mathbb{Z}_k$ parafermions possess $k(k + 1)/2$ sectors: the $\mathbb{Z}_k$ parity rule [20],

$$\lambda = m \mod k \ , \qquad \lambda \bmod (kM + 2) \ , \qquad m \bmod 2k \ , \tag{4.4}$$

relates the fractional charge $\lambda$ to the parafermion charge $m$, leading to the multiplicity of $(\lambda, m)$ pairs in (4.3). One physical motivation for the parity rule is the requirement of locality (analyticity) of all excitations w.r.t. electrons in the wave functions (cf. (2.19)) [20].

## 4.1 Partition functions

The partition functions of Read-Rezayi states have been already obtained in [20] from a physically motivated construction involving the projection from the Abelian theory with $\widehat{U(1)} \times \widehat{SU(k)}_1 \times \widehat{SU(k)}_1$ symmetry. In particular, the $\mathbb{Z}_k$ parafermionic theory for neutral excitations was described by the coset construction $\mathrm{PF}_k = \widehat{SU(k)}_1 \times \widehat{SU(k)}_1/\widehat{SU(k)}_2$.

In the following, the annulus partition functions will be found by solving the modular conditions as in section 3.2; the parafermions will be described by the standard
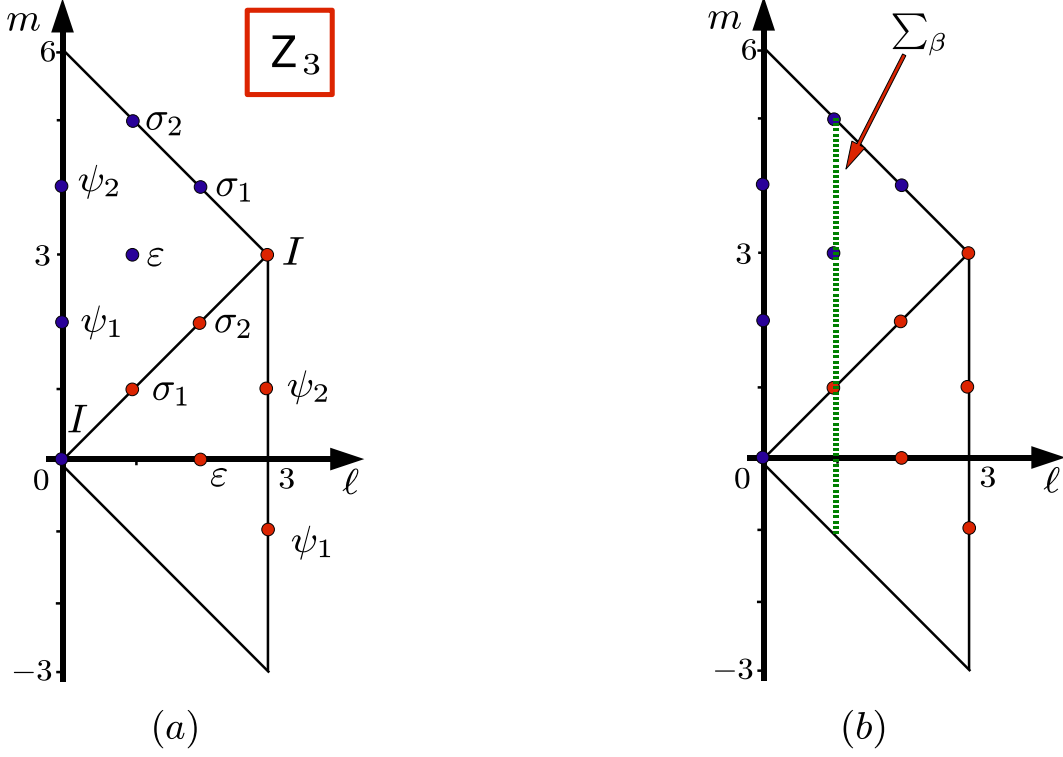
22

Figure 5: Diagram of $\mathbb{Z}_3$ parafermion fields: (a) field symbols; (b) on the green line, fields involved in $\ell = 1$ sectors of the $k = 3$ Read-Rezayi partition function.

coset, $\mathrm{PF}_k = \widehat{SU(2)}_k / \widehat{U(1)}_{2k}$, that characterizes their sector by the quantum numbers $(\ell, m)$, equal to twice the spin and spin component, respectively [41].

The dimensions of parafermionic fields $\phi_m^\ell$ are given by:

$$h_m^\ell = \frac{\ell(\ell+2)}{4(k+2)} - \frac{m^2}{4k} \, , \qquad \ell = 0, 1, \ldots, k, \qquad -\ell < m \leq \ell, \quad \ell = m \bmod 2 \, . \quad (4.5)$$

For example, the $\mathbb{Z}_3$ parafermion fields are shown in Fig. 5(a): the coset construction implies that the $m$ charge is defined modulo $2k$ [41], thus the fields are repeated once outside the fundamental $(\ell, m)$ domain (4.6) by the reflection-translation, $(\ell, m) \to (k - \ell, m + k)$,

$$\phi_m^\ell = \phi_{m-k}^{k-\ell} \, , \qquad \ell = 0, 1, \ldots, k, \qquad l < m \leq 2k - l \, . \quad (4.6)$$

The fusion rules are given by the addition of the $\widehat{SU(2)}_k$ spin and $\widehat{U(1)}_{2k}$ charge:

$$\phi_m^\ell \cdot \phi_{m'}^{\ell'} = \sum_{\ell'' = |\ell - \ell'|}^{\min(\ell + \ell', 2k - \ell - \ell')} \phi_{m+m' \bmod 2k}^{\ell''} \, . \quad (4.7)$$

23

In particular, the parafermions $\psi_j = \phi_{2j}^0$, $j = 1, \ldots, k-1$, obey Abelian fusion rules w.r.t. the index $j \mod k$. In the Read-Rezayi states, $\psi_1$ represents the neutral component of the electron and the fusion, $(\psi_1)^k = I$, describes the $k$-clustering property of the ground state wave function [11].

In order to find the annulus partition function, we need the expressions and modular transformations of parafermionic characters, denoted by $\chi_m^\ell(\tau; k)$: they obey,

$$\chi_m^\ell = \chi_{m+2k}^\ell = \chi_{m+k}^{k-\ell} , \quad m = \ell \bmod 2, \qquad \chi_m^\ell = 0 \quad m = \ell + 1 \bmod 2 . \quad (4.8)$$

The transformations can be obtained from those of $\widehat{SU(2)}_k$ and $\widehat{U(1)}_{2k}$ characters, respectively denoted by $\Theta_\ell(\tau; k)$ and $K_m(\tau, 0; 2k)$, by using the coset relation [41]:

$$\Theta_\ell(\tau; k) = \sum_{m=-k}^{k-1} K_m(\tau, 0, 2k) \, \chi_m^\ell(\tau; k) . \quad (4.9)$$

The Luttinger sectors $K_\lambda$ were described in section 3 and the $\widehat{SU(2)}_k$ characters and transformations are well known [3]: the $\widehat{SU(2)}_k$ $S$ matrix has a simpler form if we extend the domain of the index $\ell$ to $L = \ell + 1 \bmod N = 2(k+2)$, by defining, $\Theta_L = \Theta_{L+N} = -\Theta_{-L}$ (note that $\Theta_L = 0$ for $L = 0, N/2$) [28]. In the extended domain the transformation reads: $\Theta_L(-1/\tau) = -i \sum_{L' \bmod N} \exp\left(i2\pi LL'/N\right) \Theta_{L'}(\tau)/\sqrt{N}$. It follows that:

$$\chi_m^L(-1/\tau; k) = \frac{-i}{\sqrt{4k(k+2)}} \sum_{\substack{L' \\ \bmod\, 2(k+2)}} \sum_{\substack{m' \\ \bmod\, 2k}} e^{-i2\pi\frac{mm'}{2k}} e^{i2\pi\frac{LL'}{2(k+2)}} \chi_{m'}^{L'}(\tau; k) . \quad (4.10)$$

The $\mathbb{Z}_k$ parity rule (4.4) should now be used to couple the neutral characters $\chi_m^\ell$ to the charged ones, given by $K_\lambda(\tau, k\zeta; k\hat{p})$, $\hat{p} = kM+2$, in agreement with the spectrum (4.2). As in the case of hierarchical states of section 3.2, we should find the $\hat{p}(k+1)/2$ sectors of the Read-Rezayi theory within the $K_\lambda \chi_m^\ell$ tensor basis of dimension $k^2$ times larger. It is thus natural to introduce analogous sums of $k$ terms,

$$\theta_a^\ell = \sum_{\beta=1}^k K_{a+\beta\hat{p}}(\tau, k\zeta; k\hat{p}) \, \chi_{a+2\beta}^\ell(\tau; k) , \qquad \begin{array}{l} a = 0, 1, \ldots, \hat{p} - 1, \ \hat{p} = kM + 2, \\ \ell = 0, 1, \ldots, k, \\ a = \ell \bmod 2, \end{array}$$

$$(4.11)$$

that obey the parity rule (4.4) and reproduce the spectrum (4.2). Their periodicity, $\theta_{a+\hat{p}}^\ell = \theta_a^{k-\ell}$, justifies the indicated ranges for the indices and checks the value of the topological order.

The $S$ transformation of the generalized characters $\theta_a^\ell$ can be found by using the previous formulas; after returning to the $\ell$ index, it reads:

$$\theta_a^\ell(-1/\tau) = \sqrt{\frac{2}{(k+2)\hat{p}}} \sum_{a'=1}^{\hat{p}} \sum_{\ell'=0}^k e^{-i2\pi\frac{aa'M}{2\hat{p}}} \sin\left(\frac{\pi(\ell+1)(\ell'+1)}{k+2}\right) \theta_{a'}^{\ell'}(\tau), \ \ a = \ell \bmod 2,$$

$$(4.12)$$

and $\theta_a^\ell(-1/\tau)$ vanishes for $a = \ell + 1$ mod 2 (hereafter, we disregard the global phase $\propto \mathrm{Re}(\zeta^2/\tau)$ in the characters). The annulus partition function of Read-Rezayi states is given by the diagonal sesquilinear form,

$$Z_{\text{annulus}}^{\text{RR}} = \sum_{\ell=0}^{k} \sum_{\substack{a=0 \\ a=\ell \bmod 2}}^{\hat{p}-1} \left| \theta_a^\ell \right|^2 , \qquad (4.13)$$

that solves the $(S, T^2, U, V)$ conditions of section 2.2. One can check that these partition functions are equal to those found in [20].

Let us give some examples. In the Pfaffian state, the $\mathbb{Z}_2$ parafermions are the three fields of the Ising model: $\phi_0^0 = \phi_2^2 = I$, $\phi_1^1 = \phi_3^1 = \sigma$ and $\phi_2^0 = \phi_0^2 = \psi$, of dimensions $h = 0, 1/16, 1/2$, respectively. For $\nu = 5/2$, i.e. $M = 1$ in (4.1), the Pfaffian theory possesses 6 sectors. The partition function is as follows: denoting the neutral characters with the same symbol of the field and the charged ones by $K_\lambda = K_\lambda(\tau, 2\zeta; 8)$, $K_\lambda = K_{\lambda+8}$, with charge $Q = \lambda/4 + 2\mathbb{Z}$, we rewrite (4.13) as,

$$
\begin{aligned}
Z_{\text{annulus}}^{\text{Pfaffian}} &= |K_0 I + K_4 \psi|^2 + |K_0 \psi + K_4 I|^2 + |(K_1 + K_{-3})\sigma|^2 \\
&+ |K_2 I + K_{-2}\psi|^2 + |K_2 \psi + K_{-2}I|^2 + |(K_3 + K_{-1})\sigma|^2 . \quad (4.14)
\end{aligned}
$$

The first term describes the ground state and its electron excitations, such as those in $K_4 \psi$ with $Q = 1 + 2\mathbb{Z}$; in the third and sixth terms, the characters $K_{\pm 1}\sigma$ contain the basic quasiparticles with charge, $Q = \pm 1/4$, and non-Abelian fusion rules $\sigma \cdot \sigma = I + \psi$. The other sectors are less familiar: the second term contains a $Q = 0$ Ising-fermion excitation (in $K_0 \psi$) and the 4th and 5th sectors describe $Q = \pm 1/2$ Abelian quasiparticles.

The $k = 3$ Read-Rezayi state is also interesting because it is the simplest of these systems that could perform universal quantum computations by braiding non-Abelian quasiparticles [5]. It could be observable at $\nu = 13/5$, i.e $M = 1$, and possibly at $\nu = 12/5$ by charge conjugation. The 6 $\mathbb{Z}_3$ parafermion fields are listed in Fig. 5(a) with the corresponding $(\ell, m)$ labels (the complete list of their quantum numbers can be found in [20]). The characters obey: $\chi_m^\ell = \chi_{m+6}^\ell = \chi_{m+3}^{3-\ell}$. The charged sectors are given by $K_a = K_a(\tau, 3\zeta; 15)$, with charge $Q = a/5 + 3\mathbb{Z}$, and the topological order is equal to 10. The annulus partition function can be written:

$$
\begin{aligned}
Z_{\text{annulus}}^{\mathbb{Z}_3} &= \sum_{a=0,\pm 2} \sum_{\ell=0,2} \left| K_a \chi_a^\ell + K_{a+5}\chi_{a+2}^\ell + K_{a-5}\chi_{a-2}^\ell \right|^2 \\
&+ \sum_{a=\pm 1} \sum_{\ell=1,3} \left| K_a \chi_a^\ell + K_{a+5}\chi_{a+2}^\ell + K_{a-5}\chi_{a-2}^\ell \right|^2 . \quad (4.15)
\end{aligned}
$$

As in the Pfaffian case, the basic quasiparticles are represented by spin fields, $\sigma_1 K_1$, $\sigma_2 K_{-1}$, with smallest charges $Q = \pm 1/5$ and Virasoro dimensions; since these excitations have the smallest $SU(2)$ spin, $(\ell, m) = (1, \pm 1)$, we can interpret the index $\ell$ as counting the number of quasiholes in the system.

## 4.2 Coulomb blockade

The analysis of degenerate energies and conductance peaks under area variations $\Delta S$ can be obtained from the disk partition functions (4.11),

$$Z_{\text{disk}}^{(a,\ell)} \;=\; \theta_a^\ell = \sum_{\beta=1}^{k} K_{a+\beta\hat{p}}(\tau, k\zeta; k\hat{p}) \; \chi_{a+2\beta}^\ell(\tau; k) \;,$$

$$a = 1, \ldots, \hat{p} = (kM+2), \quad \ell = 0, 1, \ldots, k, \quad a = \ell \bmod 2. \quad (4.16)$$

As seen in the previous examples, each $(\ell, a)$ sector involves the parafermion fields of same $\ell$ value (along the vertical line in Fig. 5(b)), each one associated to charges mod $k\mathbb{Z}$. Therefore, adding one electron corresponds to going from $\beta \to \beta + 1$ in the corresponding sector $\theta_a^\ell$ (4.16). The distance between the conductance peaks is given by:

$$\Delta\sigma_\beta^\ell = \sigma_{\beta+1}^\ell - \sigma_\beta^\ell = \frac{\hat{p}}{k} + \frac{v_n}{v}\left(h_{a+2\beta+4}^\ell - 2h_{a+2\beta+2}^\ell + h_{a+2\beta}^\ell\right) \;, \qquad (4.17)$$

that generalizes the earlier Abelian formula (3.25).

The peak distances are modulated by the energies of neutral parafermions $h_m^\ell$ through their discrete second derivative. This is constant, $\Delta^2 h_m^\ell = -2/k$, up to discontinuities at the boundaries of the domains in the $(\ell, m)$ plane, which are the diagonals, $\ell = \pm m$, $m \bmod 2k$ (see Fig. 5(a).). Whenever $a + 2\beta + 2$ in (4.17) stays on one diagonal, the result is $\Delta^2 h_m^\ell = 1 - 2/k$; at the crossing of two diagonals, $(\ell, m) = (0,0), (k,k)$, mod $(0, 2k)$, it reads $\Delta^2 h_m^\ell = 2 - 2/k$. Therefore, the peak patterns are the following,

$$
\begin{array}{llll}
\ell = 0, k & : & \Delta\sigma = (\Delta + 2r, \Delta, \cdots, \Delta)\,, & (k) \quad \text{groups,} \\
\ell = 1, \ldots, k-1 & : & \Delta\sigma = (\Delta + r, \Delta, \cdots, \Delta + r, \Delta, \ldots, \Delta)\,, & (\ell)(k-\ell) \quad \text{groups,}
\end{array}
$$

$$\Delta = \frac{1}{\nu} - \frac{v_n}{v}\frac{2}{k} \;, \qquad r = \frac{v_n}{v} \;. \qquad (4.18)$$

In these non-Abelian Hall states, the peak patterns depend on the number of basic $\sigma_1$ quasiparticles in the bulk: for $\ell$ of them, there are groups of $\ell$ and $(k-\ell)$ equidistant peaks separated by a larger gap, $\Delta + r$, $r = v_n/v$. The patterns are symmetric by $\ell \leftrightarrow (k-\ell)$ and depends on the other quantum number $a$ only in the (irrelevant) starting point of the sequence. In particular, for the Pfaffian state $(k = 2)$, the peaks group in pairs when the number of bulk quasiparticles is even, and are equidistant when it is odd, the so called "even-odd effect" [22]. The analysis of $\chi_a^\ell$ characters also shows that there are no degenerate states in parafermionic excitations, and thus the Coulomb peaks have no multiplicities.

The peak patterns repeat periodically with period $\Delta\sigma = k/\nu = kM+2$, apart from the case $k$ even and $\ell = k/2$, where it is halved. The same results were found by the direct analysis of parafermion Hilbert space in [23][19].

The peak pattern in the ground state sector of Read-Rezayi states is actually the same as in the Jain hierarchical Hall states of section 3.2, up to a factor of 2 in
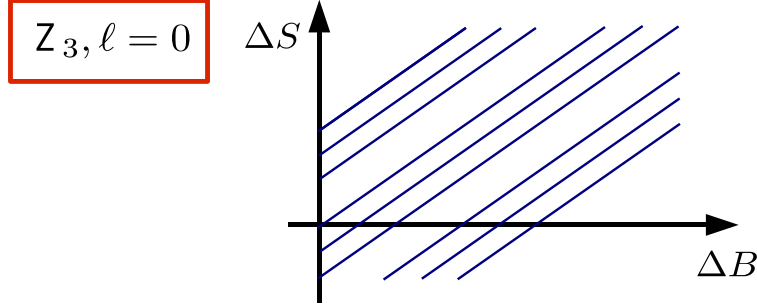
Figure 6: Coulomb peaks in the area $(S)$ and magnetic field $(B)$ plane.

the neutral energies. However, the Abelian case is characterized by specific peak multiplicities and is independent of the sector, i.e. of bulk excitations.

## 4.3 Peak patterns in the $(S, B)$ plane

We now analyze the peak patterns in the $(S, B)$ plane, i.e. by simultaneous changes of area and magnetic field. Let us first discuss $\Delta B$ changes at $\Delta S = 0$: from section 3.1, we recall that varying the field causes a chiral anomaly and a drift of all charges in the theory. The addition of one flux quantum, $\delta = S \Delta B / \phi_o = 1$ modifies the charged characters in the disk partition functions (4.16) by $K_\lambda(\tau, k\zeta; q) \to K_{\lambda+k}$, i.e. by a charge equal to the filling fraction. The spectral flow of Read-Rezayi sectors is therefore:

$$\theta_a^\ell \ \to \ \theta_{a+k}^{k-\ell} = \theta_{a-2-(M-1)k}^\ell \ . \tag{4.19}$$

Namely, the sector $\ell$ goes into itself with a shift of the $a$ index: the peak pattern already found for $S$ variations at $\Delta B = 0$ repeats itself at $\Delta B = \phi_o/S$ with an upward translation (see Fig. 6). This continues for $\delta = 2, \ldots$: eventually the sector $\ell$ goes to the $(k - \ell)$ one, with the same pattern, and then back to itself.

This behavior of peaks in $B$ was also found for the Laughlin states and actually holds in full generality: the peaks only depend on the combined variation $(\sigma - \delta)$. The proof is very simple: the magnetic field does not couple to the neutral characters, that are unchanged; since they determine the peak modulations, the pattern remains the same. The only effect is a rigid shift of the $\Delta S$ peak pattern at $\Delta B = 0$.

In general, a magnetic flux induces a localized charge excitation inside the Hall droplet, but this has to combine with a neutral excitation to form a physical state: in non-Abelian states, there might be several possibilities. The result of the present analysis is that neutral parts are not created and the $\ell$ sector does not change: there is a drift of states within the same sector or the conjugate $(k - \ell)$. One could naively think that $\Delta B > 0$ would create the lowest charge quasiparticle $\sigma_1$, but this would require a transition $(\Delta \ell, \Delta m) = (1, 1)$ that cannot be induced in isolated droplets within the relativistic CFT description. Maybe it could be realized by engineering a

27

antidot inside the disk and by charging it, if further non-relativistic effects are taken into account [22].

In conclusion, the peak patterns in the $(S, B)$ plane are not different from those on the $S$ axis. In ref. [24], it was observed that, for $\nu > 2$, increasing $B$ causes a depletion of electrons in the second Landau level, that go into available states in the first level; this is another effect that rigidly translate upwards the peak patterns in the $B$ plane, i.e. it is of the same sign as the spectral flow described here.

## 4.4  Bulk-edge relaxation

In reference [19], a mechanism for relaxation of edge excitations has been proposed. While the electric charge is locally conserved at the edge, the neutral charge is (expected to be) only globally conserved: therefore, a (slow-time) process can be conceived in which neutral excitations at edge and bulk fuse together thus achieving a lower energy state at the edge. In this mechanism, the electron added at the boundary decays into another excitation with same charge but different neutral content. This process is possible whenever the theory possess two or more excitations with same electric charge but different neutral parts, among which the relaxation transition can take place.

In non-Abelian theories, there are necessarily many-to-one combinations of neutral and charged parts. Consider the following example of fusion rules:

$$\phi_1 \cdot \phi_2 = \psi + \psi' . \tag{4.20}$$

Both $\phi_1, \phi_2$ fields contain charged and neutral components, and electric charge is conserved: thus, the fields $\psi, \psi'$ have same electric charge but different neutral parts. A possible relaxation at the edge is, $\psi \to \psi'$, by absorption of one neutral bulk excitation, call it $\varepsilon$, via the fusion, $\psi \cdot \varepsilon = \psi' + \cdots$. It is rather natural to expect that the $\varepsilon$ field exists in the theory.

In the Read-Rezayi states, the parafermionic parts can change as follows: the $m$ quantum number should stay fixed because it is related to the charge by the $\mathbb{Z}_k$ parity rule, thus $\ell$ can change by an even integer: the minimal value is $(\Delta \ell, \Delta m) = (\pm 2, 0)$. These transitions should reduce the value of the edge energy, i.e. of $h_m^\ell$. The plot in Fig. 7 shows that the smallest values are found on the diagonals $m = \pm \ell \mod 2k$: therefore, the peak patterns are analyzed starting from the low-lying states $(\ell, m = \pm \ell)$.

Let us consider for example the initial state $(\ell, m) = (1, 1)$, as drawn in the parafermion diagram of Fig. 8. The first peak is found by comparing with the energy levels of the next term in the same $\ell = 1$ sector, i.e in $\theta_1^1$, which is $(1, 3)$ (joined by a green line in Fig. 8); then the higher energy of the latter allows the relaxation, $(1, 3) \to (3, 3)$, (red line), bringing to the $\ell = 3$ sector. The next peak is therefore obtained by comparing $(3, 3)$ to $(3, -1)$, followed by the relaxation $(3, -1) \to (1, -1)$; the next peak compares $(1, -1)$ with $(1, 1)$ and so on.

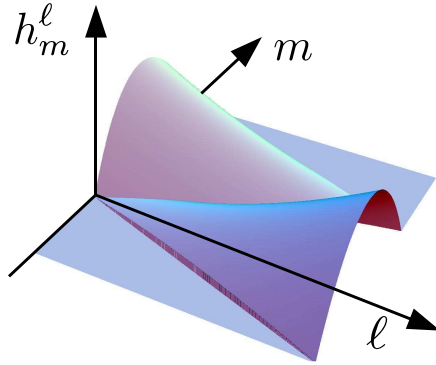Figure 7: Conformal dimension $h_m^\ell$ of parafermion fields.

Therefore, the peak patterns with relaxation are obtained by comparing points in the $(\ell, m)$ plane that are reached by zig-zag walking along the diagonals, that correspond to minimal edge energies (Fig. 8). The relaxations are achieved by fusing the edge fields with the $(\ell, m) = (2, 0)$ parafermion that is always present in the spectrum (higher $\Delta\ell$ transitions have larger energies and are never reached). The peak distances $\Delta\sigma$ are computed as in section 4.2:

$$\Delta\sigma = \sigma_{\beta+1}^{\ell\pm2} - \sigma_\beta^\ell = \frac{\hat{p}}{k} + \frac{v_n}{v} \left( h_{2\beta+4}^{\ell\pm2} - h_{2\beta+2}^{\ell\pm2} - h_{2\beta+2}^\ell + h_{2\beta}^\ell \right) \ , \tag{4.21}$$

where the $\ell\pm2$ point is along the zig-zag path. These derivatives are independent of $\ell$ and their values are already known: the separations $\Delta\sigma$ acquire the extra contribution $v_n/v$ when the midpoint $m = 2\beta + 2$ stays on a diagonal.

The resulting peak patterns are the following,

$$\begin{array}{llll} k \text{ even, any } \ell : & \left(\frac{k}{2}\right) \ \left(\frac{k}{2}\right) & \text{groups,} \\ k \text{ odd, any } \ell : & \left(\frac{k+1}{2}\right) \ \left(\frac{k-1}{2}\right) & \text{groups.} \end{array} \tag{4.22}$$

They do not depend on the (starting) $\ell$ value; in particular, the even-odd effect in the Pfaffian state doe not take place in presence of bulk-edge relaxations. Form the experimental point of view, relaxations could take place on long time scales, and thus be controlled, but this is still unclear [19].

Let us remark that in the Jain hierarchical states of section 3, bulk-edge relaxations corresponding to change of sectors $\theta_a$ (3.23) are not possible, because any charge component, $K_\lambda$, appears only once in the spectrum (cf.(3.24)), so it is uniquely coupled to a neutral part.

# 5   Discussion and conclusions

In this paper, we described the CFT partition functions of quantum Hall states: we introduced and solved the modular invariance conditions of the annulus geometry,
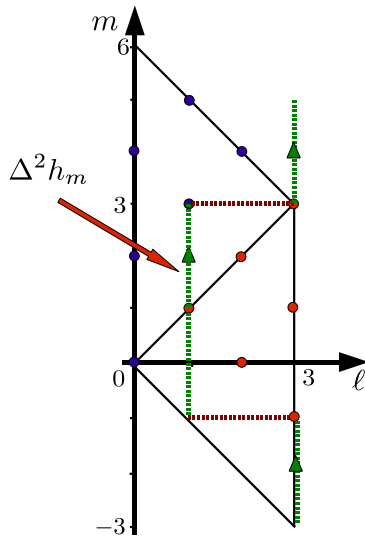
Figure 8: Zig-zag path connecting the $\mathbb{Z}_3$ parafermion fields involved in the evaluation of Coulomb peaks with relaxation: the read segments are relaxation transitions.

and obtained the disk expressions describing isolated Hall droplets. We stressed that the partition functions are defining quantities of rational CFTs: they clearly display the sectors of the Hilbert space, and account for the multiplicities of states and the fusion rules.

We used the disk partition functions to readily analyze the degenerate edge states leading to Coulomb blockade conductance peaks. We found that the peak patterns can be non-trivial whenever the edge excitations involve neutral components; generically, the modulation in the peak distances are of the order $O(v_n/v)$, the ratio of velocities of neutral and charged excitations.

The peak modulations can occur both in Abelian and non-Abelian Hall states, but they can have different characteristics. In the case of the Abelian Jain hierarchical states, the patterns are independent of the presence of quasiparticles in the bulk and bulk-edge relaxation phenomena are not possible. Furthermore, the multiplicities of edge excitations, due to the extended symmetry of the multicomponent edge, could be observed by a careful analysis of the peak sequences. Two alternative theories for the Jain states were also considered, that have no multiplicities.

The Coulomb peak patterns of non-Abelian Read-Rezayi states do depend on the presence of bulk quasiparticles; however, bulk-edge relaxation processes could be possible that would erase such dependence. We remark that relaxation phenomena are generically possible in non-Abelian states.

Although the modulation of conductance peaks is not by itself a characteristic feature of non-Abelian statistics of excitations, the detailed features of the patterns can test the CFT description, in particular the qualitative properties of its Hilbert

30

space. Isolated droplets, such as those involved in Coulomb blockade experiments, can provide rather clean experimental signals, that may not reveal many features of Hall states but are nevertheless very interesting. In particular, the fine structure of conductance peaks in the Jain states is a signature of the composite edge structure: from its lifting, one could check additional interactions in the Hamiltonian, inter-edge couplings and edge reconstruction effects etc. [32].

The chiral partition functions are useful in many contexts, besides the study of Coulomb blockade presented in this paper. In the future, we want to use them for further model building of non-Abelian states and for the description of the topological entanglement entropy of Hall droplets [6]. The determination of $Z_{\text{disk}}$ for other relevant Hall states, such the Ardonne-Schoutens non-Abelian spin singlet states [42], will also presented in another publication.

While writing this report, we received the paper [43] where Coulomb blockade patterns were also found for several Hall states.

# A  Modular forms and functions

In this appendix, we briefly review some of the properties of modular invariant functions [17]. Form section 2.2, we recall that annulus partition functions of quantum Hall states should contain fermionic excitations and be invariant under the $S$ and $T^2$ transformations. They generate the subgroup $\Gamma_\theta \subset \Gamma$ which is isomorphic to $\Gamma^0(2) = T\Gamma_\theta T^{-1} = \{(a,b,c,d) \in \Gamma | b = 0 \bmod 2\}$. The transformations $ST^2S$ and $S$ generate the subgroup $\Gamma(2)$ of the modular group $\Gamma = SL(2,\mathbb{Z})/\mathbb{Z}_2$ of transformations (2.8) which are subjected to the conditions $(a,d)$ odd and $(b,c)$ even.

In the study of the functions on the torus, one naturally encounters the modular forms $F(z)$, which transform under (2.8) as:

$$F\left(\frac{a\tau + b}{c\tau + d}\right) = \varepsilon \ (c\tau + d)^\beta F(\tau) \ , \tag{A.1}$$

where $\varepsilon$ is a phase and $\beta$ is the weight of the modular form. A modular function has weight $\beta = 0$. The simplest example of a modular form is the Dedekind function,

$$\eta(\tau) = q^{1/24} \prod_{k=1}^\infty (1 - q^k) = q^{1/24} \sum_{n \in \mathbb{Z}} (-1)^n q^{\frac{1}{2}n(3n+1)} \ , \qquad q = \mathrm{e}^{i2\pi\tau} \ . \tag{A.2}$$

The last equality is known as Euler's pentagonal identity, and it is a consequence of Jacobi's triple product identity [3]:

$$\prod_{n=1}^{\infty}(1-q^n)(1+q^{n-1/2}w)(1+q^{n-1/2}w^{-1}) = \sum_{n\in\mathbb{Z}}q^{n^2/2}w^n \ , \tag{A.3}$$

after replacing in (A.3) $q \to q^3$ and $w \to -q^{-1/2}$. Under the two generators $T : \ \tau \to \tau+1$ and $S : \ \tau \to -1/\tau$ of the modular group, the transformations laws of $\eta(\tau)$ are,

$$T : \ \eta(\tau+1) \ = \ \mathrm{e}^{2i\pi/24}\eta(\tau) \ , \tag{A.4}$$

$$S : \ \eta(-1/\tau) \ = \ (-i\tau)^{1/2}\eta(\tau) \ . \tag{A.5}$$

The proof of Eq.(A.4) is straightforward, and that of Eq.(A.5) follows from the application of Poisson's resummation formula,

$$\sum_{n\in\mathbb{Z}}f(n) \ = \ \sum_{p\in\mathbb{Z}}\int_{-\infty}^{+\infty}dx\ f(x)\ \mathrm{e}^{2i\pi px} \ , \tag{A.6}$$

to the r.h.s. of Eq.(A.2). Under a general transformation (2.8) we therefore have

$$\eta\left(\frac{a\tau+b}{c\tau+d}\right) = \varepsilon_A\,(c\tau+d)^{1/2}\,\eta(\tau) \ , \tag{A.7}$$

where $\varepsilon_A$ is a $24th$ root of unity. Thus, the Dedekind is a modular form of weight $1/2$.

Another important example of a modular form considered in section two is the theta function with characteristics $a$ and $b$, which is a map $\mathcal{F}\times\mathbb{C}\to\mathbb{C}$ defined by:

$$\Theta\begin{bmatrix}a\\b\end{bmatrix}(\zeta|\ \tau) = \sum_{n\in\mathbb{Z}}\mathrm{e}^{\,i\pi\tau(n+a)^2 + i2\pi(n+a)(\zeta+b)} \ . \tag{A.8}$$

In the case of Laughlin fluids, one has $b = 0$ and $a = \lambda/p$, with $\lambda = 1, 2, \ldots, p$. The transformation properties of (2.15), Eq.(2.16) follow easily from its definition. The only non-trivial calculation regards the $S$ transformation, which can be done following the example of the Dedekind function. It is also easy to verify that (A.8) is a modular form of weight $1/2$. It follows that the quotient of the theta function (A.8) by the Dedekind function (A.2) is a modular function. In section 2 we introduced the notation:

$$K(\tau,\zeta;q) = \frac{1}{\eta}\Theta\begin{bmatrix}\lambda/q\\0\end{bmatrix}(\zeta|q\tau) \ . \tag{A.9}$$

# References

[1] X. G. Wen, *Quantum Field Theory of Many-body Systems*, Oxford Univ. Press (2007), Oxford.

[2] A. Stern, *Anyons and the quantum Hall effect - a pedagogical review*, Ann. Phys. **323** (2008) 204.

[3] P. Di Francesco, P. Mathieu and D. Senechal, *Conformal Field Theory*, Springer (1999), Berlin.

[4] P. Bonderson, A. Kitaev, and K. Shtengel, *Detecting Non-Abelian Statistics in the =5/2 Fractional Quantum Hall State* , Phys. Rev. Lett. **96** (2006) 016803; W. Bishara, P. Bonderson, C. Nayak, K. Shtengel, J. K. Slingerland, *The non-Abelian Interferometer* , arXiv:0903.3108.

[5] C. Nayak, S. H. Simon, A. Stern, M. Freedman and S. Das Sarma, *Non-Abelian anyons and topological quantum computation*, Rev. Mod. Phys. **80** (2008) 1083.

[6] P. Fendley, M. P. A. Fisher and C. Nayak, *Topological Entanglement Entropy from the Holographic Partition Function*, J. Statist. Phys. **126** (2007) 1111.

[7] E. Verlinde, *Fusion rules and modular transformations in 2D conformal field theory*, Nucl. Phys. **B300** (1988) 360.

[8] E. Witten, *Quantum field theory and the Jones polynomial*, Commun. Math. Phys. **121** (1989) 351.

[9] R. Dijkgraaf and E. Verlinde, *Modular invariance and the fusion algebra*, Nucl. Phys. **B** (Proc. Suppl.) **5 B** (1988) 87; G. Moore and N. Seiberg, *Polynomial equations for rational conformal field theories*, Phys. Lett. **B 212** (1988) 451; *Naturality in conformal field theory*, Nucl. Phys. **B 313** (1989) 16; for a review, see: *Lectures on RCFT*, proceedings of the 1989 Banff Summer school, H. C. Lee ed., Plenum Press (1990), New York.

[10] N. Read, *Excitation structure of the hierarchy scheme in the fractional quantum Hall effect*, Phys. Rev. Lett. **65** (1990) 1502; J. Fröhlich and A. Zee, *Large scale physics of the quantum hall fluid*, Nucl. Phys. **B 364** (1991) 517; X.-G. Wen and A. Zee, *Classification of Abelian quantum Hall states and matrix formulation of topological fluids*, Phys. Rev. **B 46** (1992) 2290.

[11] N. Read and E. Rezayi, *Beyond paired quantum Hall states: Parafermions and incompressible states in the first excited Landau level*, Phys. Rev. **B 59** (1999) 8084.

[12] A.B. Zamolodchikov and V.A. Fateev, *Parafermionic Currents in the Two-Dimensional Conformal Quantum Field Theory and Selfdual Critical Points in Z(n) Invariant Statistical Systems*, Sov. Phys. JETP **62** (1985) 215.

[13] A. Cappelli, C. A. Trugenberger and G. R. Zemba, *Stable hierarchical quantum Hall fluids as $W_{1+\infty}$ minimal models*, Nucl. Phys. **B 448** (1995) 470; for a review, see: *$W_{1+\infty}$ minimal models and the hierarchy of the quantum Hall effect*, Nucl. Phys. *(Proc. Suppl.)* **B 45A** (1996) 112.

[14] A. Lopez and E. Fradkin, *Universal structure of the edge states of the fractional quantum Hall states*, Phys. Rev. **B 59**, (1999) 15323.

[15] J. K. Jain, *Composite Fermions*, Cambridge Univ. Press (2007), Cambridge.

[16] M. H. Freedman, A. Kitaev and Z. Wang, *Simulation of topological field theories by quantum computers*, Commun. Math. Phys. **227** (2002) 587; A. Kitaev, *Anyons in an exactly solved model and beyond*, Ann. Phys. **321** (2006) 2; E. Rowell, R. Stong and Z. Wang, *On Classification of Modular Tensor Categories*, preprint arXiv:0712.1377, Commun. Math. Phys. in press; L. Fidkowski, M. Freedman, C. Nayak, K. Walker and Z. Wang, *From string nets to nonabelions,* Commun. Math. Phys. **287** (2009) 805.

[17] A. Cappelli and G. R. Zemba, *Modular invariant partition functions in the quantum Hall effect*, Nucl. Phys. **B 490** (1997) 595.

[18] A. Cappelli, L. S. Georgiev and G. R. Zemba, *Coulomb blockade in hierarchical quantum Hall droplets*, J. Phys. **A 42** (2009) 222001.

[19] R. Ilan, E. Grosfeld, K. Schoutens and A. Stern, *Experimental signatures of non-Abelian statistics in clustered quantum Hall states*, Phys. Rev. **B 79** (2009) 245305.

[20] A. Cappelli, L. S. Georgiev and I. T. Todorov, *Parafermion Hall states from coset projections of Abelian conformal theories*, Nucl. Phys. **B 599** (2001) 499.

[21] C. de C. Chamon, D. E. Freed, S. A. Kivelson, S. L. Sondhi, and X. G. Wen, *Two point-contact interferometer for quantum Hall systems*, Phys. Rev. **B 55**, (1997) 2331.

[22] A. Stern and B. I. Halperin, *Proposed Experiments to Probe the Non-Abelian $\nu = 5/2$ Quantum Hall State*, Phys. Rev. Lett. **96** (2006) 016802.

[23] R. Ilan, E. Grosfeld and A. Stern, *Coulomb Blockade as a Probe for Non-Abelian Statistics in Read-Rezayi States*, Phys. Rev. Lett. **100** (2008) 086803.

[24] Y. Zhang, D. T. McClure, E. M. Levenson-Falk, C. M. Marcus, L. N. Pfeiffer, K. W. West, *Distinct Signatures For Coulomb Blockade and Aharonov-Bohm Interference in Electronic Fabry-Perot Interferometers* , Phys. Rev. **B 79**, (2009) 241304.

[25] S. Elitzur, G. Moore, A. Schwimmer and N. Seiberg, *Remarks on the canonical quantization of the Chern-Simons-Witten theory*, Nucl. Phys. **B 326** (1989) 108; G. Dunne, R. Jackiw and C. Trugenberger, *Chern-Simons theory in the Schrödinger representation*, Ann. Phys. **194** (1989) 197.

[26] A. Cappelli, G. V. Dunne, C. A. Trugenberger and G. R. Zemba, *Conformal symmetry and universal properties of quantum Hall states* , Nucl. Phys. **B 398** (1993) 531.

[27] L. S. Georgiev, *A universal conformal field theory approach to the chiral persistent currents in the mesoscopic fractional quantum Hall states*, Nucl. Phys. **B 707** (2005) 347.

[28] A. Cappelli, C. Itzykson and J. B. Zuber, *Modular Invariant Partition Functions in Two-Dimensions*, Nucl. Phys. **B 280** (1987) 445.

[29] R. B. Laughlin, *Anomalous Quantum Hall Effect: An Incompressible Quantum Fluid with Fractionally Charged Excitations*, Phys. Rev. Lett. **50** (1983) 139; for a review see: R. B. Laughlin, *Elementary Theory: the Incompressible Quantum Fluid*, in R. A. Prange, S. M. Girvin, *The Quantum Hall Effect*, Springer Verlag (1990), Berlin.

[30] C. Itzykson, *Level one Kac-Moody characters and modular invariance*, Nucl. Phys. **B** (Proc. Suppl.) **5 B** (1988) 150.

[31] M. Grayson, D. C. Tsui, L. N. Pfeiffer, K. W. West, and A. M. Chang, *Continuum of Chiral Luttinger Liquids at the Fractional Quantum Hall Edge*, Phys. Rev. Lett. **80** (1998) 1062.

[32] See e.g.: D. Orgad and O. Agam, *Correlated Tunneling and the Instability of the Fractional Quantum Hall Edge*, Phys. Rev. Lett. **100** (2008) 156802.

[33] A. Cappelli, C. A. Trugenberger and G. R. Zemba, *Infinite symmetry in the quantum Hall effect*, Nucl. Phys. **B 396** (1993) 465; for a review, see: A.Cappelli, G.V.Dunne, C.A.Trugenberger and G.R.Zemba, *Symmetry aspects and finite-size scaling of quantum Hall fluids*, Nucl. Phys. **B** (Proc. Suppl.) **33 C** (1993) 21; S. Iso, D. Karabali and B. Sakita, *One-dimensional fermions as two-dimensional droplets via Chern-Simons theory*, Nucl. Phys. **B 388** (1992) 700; *Fermions in the lowest Landau level. Bosonization, W-infinity algebra, droplets, chiral bosons*, Phys. Lett. **B 296** (1992) 143.

[34] V. Kac and A. Radul, *Quasifinite highest weight modules over the Lie algebra of differential operators on the circle*, Commun. Math. Phys. **157** (1993) 429; H. Awata, M. Fukuma, Y. Matsuo and S. Odake, *Representation theory of the W(1+infinity) algebra*, Prog. Theor. Phys. (Supp.) **118** (1995) 343; E. Frenkel, V. Kac, A. Radul and W. Wang, $W_{1+\infty}$ *and* $\mathcal{W}(gl_N)$ *with central charge N*, Commun. Math. Phys. **170** (1995) 337.

[35] A. Cappelli and G. R. Zemba, *Hamiltonian formulation of the* $W_{1+\infty}$ *minimal models*, Nucl. Phys. **B 540** (1999) 610.

[36] M. Huerta, $\widehat{U(1)} \times \widehat{SU(m)}_1$ *theory and* $c = m$ $W_{1+\infty}$ *minimal models in the hierarchical quantum Hall effect,* Int. J. Mod. Phys. **A 15** (2000) 915.

[37] R. L. Willett, L. N. Pfeiffer and K. W. West, *Measurement of filling factor 5/2 quasiparticle interference: observation of charge e/4 and e/2 period oscillations*, preprint arXiv:0807.0221; D. Ferraro, A. Braggio, M. Merlo, N. Magnoli, and M.

Sassetti, *Relevance of Multiple Quasiparticle Tunneling between Edge States at =p/(2np+1)*, Phys. Rev. Lett. **101** (2008) 166805.

[38] G. Moore and N. Read, *Nonabelions in the fractional quantum hall effect*, Nucl. Phys. **B 360** (1991) 362.

[39] H. C. Choi, W. Kang, S. Das Sarma and L. N. Pfeiffer and K. W. West, *Fractional Quantum Hall Effect in the Second Landau Level* , Phys. Rev. **B 77** (2008) 081301.

[40] N. Read and D. Green, *Paired states of fermions in two-dimensions with breaking of parity and time reversal symmetries, and the fractional quantum Hall effect*, Phys. Rev. **B 61** (2000) 10267.

[41] D. Gepner and Z. Qiu, *Modular invariant partition functions for parafermionic field theories*, Nucl. Phys. **B 285** (1987) 423.

[42] E. Ardonne and K. Schoutens, *New Class of Non-Abelian Spin-Singlet Quantum Hall States*, Phys. Rev. Lett. **82** (1999) 5096; E. Ardonne, N. Read, E. Rezayi, K. Schoutens, *Non-Abelian spin-singlet quantum Hall states: wave functions and quasihole state counting*, Nucl. Phys. **B 607** (2001) 549.

[43] P. Bonderson, C. Nayak, K. Shtengel, *Coulomb Blockade Doppelgängers in Quantum Hall States*, preprint arXiv:0909.1056.

[44] M. I. Knopp, *Modular Functions in Analytic number Theory*, Markham Publ. Co. (1970), Chicago.